GROWTH AND CHARACTERIZATION OF CARBON NANOTUBES OVER Co-Mo/MgO CATALYSTS

A Thesis Submitted to
The Graduate School of Engineering and Sciences of
İzmir Institute of Technology
In Partial Fulfillment of the Requirements for the Degree of

MASTER OF SCIENCE

in Physics

by

Atike İNCE

July 2010
IZMIR

We approve the thesis of **Atike İNCE**

_____
Assist. Prof. Dr. Yusuf SELAMET
Supervisor

_____
Assoc. Prof. Dr. Selahattin YILMAZ
Co-Supervisor

_____
Prof. Dr. Serdar ÖZÇELİK
Committee Member

_____
Assoc. Prof. Dr. R. Tuğrul SENGER
Committee Member

_____
Assoc. Prof. Dr. Salih OKUR
Committee Member

12 July 2010

_____
Prof. Dr. Nejat BULUT
Head of the Department of Physics

_____
Assoc. Prof. Dr. Talat YALÇIN
Dean of the Graduate School of
Engineering and Sciences

ACKNOWLEDGEMENTS

First, I would like to thank my advisor Assist. Prof. Yusuf Selamet, for his continuous support during the master program. He was always very positive, helpful and patient. I learnt a lot from him and I could not have finished this thesis without his encouragement and constant guidance. It has been an honor to work with him for me.

A special thank goes to my co-advisor Assoc. Prof. Selahattin Yilmaz. Working with him and his group was a great experience for me. He taught me a lot of things about catalysts and he spent a lot of time for my project. Now, I could not remember how many times we searched literature together. I will always be gratefull for his help.

Besides my advisors, I would like to thank also other members of my thesis defense committee Assoc. Prof. Salih Okur, Assoc. Prof. R. Tugrul Senger and Prof. Serdar Ozcelik for helpful comments and giving suggestions. I want to thank to J. Brites of Horiba Scientific for Raman analysis and IYTE Material Research Center staff for SEM and TGA analysis.

I thankfully acknowledge TUBITAK for master scholarship.

I am very thankful to my lab mates at Carbon Nanostructure Laboratory Meral Aksak, Serap Kır and Deniz Söylev for their warm friendship and help. Being a physicist was a bit difficult in a chemistry laboratory, so I am also very thankful my lab mates at Catalyst Design and Reaction Engineering Laboratory Can Okan Depboylu, Emre Kılıç and Okan Akın for their help during my study.

Thanks to each of my friends at Izmir Institute of Technology for providing a great atmosphere and a wonderful workplace. We have unforgettable memories at the end of two years and now each of them is very important for me. Especially, Hale Sert, Nesli Yagmurcukardes and Derya Atac have always been by my side and shared my all feelings.

Personally, my special thanks go to some special people Esra Aydin, Sebnem Aksu and Uygar Boztepe for their good heart and love. I feel very lucky to have them in my life.

Last, but most importantly, I would like to thank my precious family: my mother Zehra Ince and my father Kaya Ince for their ceaseless support, motivation and love in all my life and believing in me. I need them always by my side.

ABSTRACT

GROWTH AND CHARACTERIZATION OF CARBON NANOTUBl OVER Co-Mo/MgO CATALYSTS

This thesis work is focused on synthesis of high quality and high yield Carbon nanotubes by methane decomposition catalytic chemical vapor deposition method on Co-Mo/MgO catalyst prepared by gel-combustion method. Catalyst contained weight %1.06 Co and weight %0.86 Mo having a molar ratio of Co:Mo:MgO;0.5:0.25:10. CNTs were grown in a quartz tube.

In this study, three different growth conditions were examined. Argon, hydrogen or mixture of two gases were added to methane during growth. And for all of the three growth conditions, four different pretreatment processes were investigated. Pretreatment lasted for one hour at 850 ^{o}C. Firstly hydrogen effect was examined with 200 sccm flow rate, then argon effect was examined with again 200 sccm flow rate. And the third pretreatment included both argon and hydrogen gases flow together. For these three pretreatment conditions cooling and heating processes also took place with the same gas rates. However, the last pretreatment condition was carried out with hydrogen gas at 850 ^{o}C for just one hour, and for heating and cooling processes argon was used. The highest quality CNTs were sythesized under pure hydrogen atmosphere for both pretreatment and growth processes.

Then, three different H_2 flow rates were investigated; 100, 150 and 200 sccm. High hydrogen flow rate during growth was better for CNT growth in terms of quality.

Growth temperature was performed as another important parameter. Four different temperatures were investigeted; 850 ^{o}C, 900 ^{o}C, 950 ^{o}C and 1000 ^{o}C. With increasing growth temperatures, structural quality increased and tangled CNTs formation decreased. It was found that 950 ^{o}C was the optimum growth tempertaure to obtain high yield of CNT.

Finally, the growth time effect on CNT growth was examined for four different growth times; 10, 20, 30 and 40 minutes and the results showed that amount of CNTs increased with increasing time and CNTs became longer and graphitization was higher at longer growth times. Disorder also decreases with increasing time.

ÖZET

Co-Mo/MgO KATALİZLER ÜZERİNE KARBON NANOTÜP BÜYÜTÜLMESİ VE KARAKTERİZASYONU

Bu tez çalışması, yüksek saflıkta ve yüksek verimde karbon nanotüplerin metan dekompozisyonu termal kimyasal buhar biriktirme tekniği ile yakma yöntemi ile hazırlanmış Co-Mo/MgO kataliz üzerinde sentezlenmesine odaklanmıştır. Kataliz %1.06 Co, %0.86 Mo içermektedir ve maddelerin kataliz içindeki molar oranı Co:Mo:MgO;0.5:0.25:10 dur.

Bu çalışmada, üç farklı büyütme koşulu incelenmiştir. Argon, hidrojen ya da bu iki gazın karışımı büyütme süresince metana eklenmiştir. Her üç büyütme koşulu için dört farklı önişlem süreci incelenmiştir. Önişlem süreci 850 ^{o}C de 1 saat sürdürülmüştür. İlk olarak 200 sccm akış hızında hidrojen etkisi incelenmiştir, daha sonra 200 sccm akış hızında argon etkisi incelenmiştir. Üçüncü önişlem süreci her iki gazı bir arada içermektedir. Bu üç önişlem süreci için ısıtma ve soğutma işlemlerinde önişlem süresince yer alan gaz aynı akış hızıyla sisteme gönderilmiştir. Ancak, dördüncü önişlem süreci diğerlerinden farklıdır. Bu sefer, önişlem süreci hidrojen gazı ile 850 ^{o}C de sadece bir saat yapılmıştır ve ısıtma ve soğutma işlemlerinde argon gazı yer almıştır. Sonuç olarak, en yüksek kalitede karbon nanotüpler hem önişlem hem büyütme süreçlerinde saf hidrojen ortamında sentezlenmiştir.

Daha sonra üç farklı hidrojen akış hızı incelenmiştir; 200 sccm, 150 sccm ve 100 sccm. ve yüksek akış hızında hidrojen, kalite açısından karbon nanotüp büyütülmesinde daha iyidir.

Büyütme sıcaklığı diğer bir parametre olarak uygulanmıştır. Dört farklı büyütme sıcaklığı incelenmiştir; 850 ^{o}C, 900 ^{o}C, 950 ^{o}C ve 1000 ^{o}C. Azalan büyütme sıcaklığıyla yapısal kalite düşmüş ve iç içe geçmiş karbon nanotüpler meydana gelmiştir. Verim açısından optimum sıcaklığın 950 ^{o}C olduğu görülmüştür.

Son olarak, büyütme süresinin etkisi dört farklı büyütme süresi için incelenmiştir; 10, 20, 30, 40 dakika ve karbon nanotüp yoğunluğu artan süre ile artmış, daha uzun karbon nanotüpler oluşmuş ve daha uzun büyütme sürelerinde daha yüksek grafitizasyon elde edilmiştir. Süre ile düzensizlik azalmıştır.

To my Lovely Family

TABLE OF CONTENTS

LIST OF FIGURES

LIST OF TABLES

CHAPTER 1

INTRODUCTION

Carbon nanotube (CNT) is an interesting form of pure carbon, which occurs when a graphene sheet rolled into a cylinder, both ends of the cylinder may be capped with a half of fullurene molecule. Carbon nanotubes have caught scientists attention with its special properties since their detailed observation TEM by Iijima in 1991 which started a new era of research. Large number of studies have been done on CNT synthesis and characterization. CNTs have been used and showed as viable potential in many applications.

Some of carbon nanotube's excellent physical properties are high aspect ratio, high Young modulus, high tensile strenght, high thermal and electrical conductivity (Salvetat, et al. 1999). Because of their high young modulus and low weigth they are useful as reinforcing agents in composite materials and in a variety of applications such as sensors, field emission devices, flat panel displays, energy storage, electrochemical devices and electronic devices (Paradise, et al. 2006).

Carbon nanotubes divide into two groups; single wall carbon nanotubes (SWNTs) and multi wall carbon nanotubes (MWNTs) depending on number of concentric graphene cylinder that tube contains (Dresselhaus, et al. 2001). A SWNT can be classified as three types with respect to the orientation of the six-membered carbon ring (hexagon) relative to the axis of the nanotube; chiral, zigzag or armchair. Chiral vector of tube defines its electronic band structure. Hence, a CNT can be semiconducting or metallic (Dresselhaus, et al. 2004). Zigzag nanotubes can be semiconducting or metallic depending on n,m indices ($C_h=n\vec{a}_1+m\vec{a}_2$) , all armchair nanotubes are metallic nanotubes (Saito, et al. 1992).

There are three main methods to produce CNTs. These are arc discharge, laser vaporization and chemical vapor deposition (CVD) methods (Baddour and Briens, 2005). Among these, CVD method is suitable for mass production. In this method an energy source such as a plasma, a resistive heater or a furnace is used to transfer energy to a gas phase carbon precursor and carbon deposition on metal catalysts results in carbon nanotube formation.

Catalyst material is very important for CNT growth. Transition metals are appropriate for CNT growth but especially Fe, Co, Ni are the best ones according to many researchers. These metal particles are generally supported by an inorganic porous material to provide high surface area for active component. There are many methods to produce catalyst. Impregnation, precipitation, combustion and sol-gel are most common ones. Gel-combustion method has some advantages; it gives high specific surface area and good dispersion of the active sites for catalyst (Rashidi, et al. 2007).

The aim of this work to sythesize effective Co-Mo/MgO catalyst particles by gel-combustion method and then grow high quality and large scale CNTs by optimizing CNT growth parameters by methane thermal chemical vapor deposition. Pretreatment and growth atmosphere gas composition, hydrogen flow rate, growth temperature and growth time are studied parameters in this study. This thesis consists of six chapters. The first one is a general information about carbon nanotubes and content of the thesis, Chapter 2 gives information about carbon nanotubes, their structure, discovery, types and growth methods with details. In Chapter 3, catalyst materials used for CNT growth are reviewed. Catalyst active component and support material and general catalyst preparation methods for CNT synthesis are explained and also literature survey of widely used catalyst materials for CNT growth is given as a table. Chapter 4 includes Co-Mo/MgO catalyst prepation by gel-combustion method, CNT production on this catalyst by chemical vapor deposition and common characterization techniques. All experimental results are given and discussed in Chapter 5 and conclusions of this study are given at Chapter 6 in the final chapter.

CHAPTER 2

CARBON NANOTUBES

2.1. Carbon Structures

Carbon is one of the special elements in the periodic table, in terms of the number of compounds. It can make single, double, and triple bonds. Due to the types of bonds it can form and the number of elements it can join in bonding, it may form an infinite number of compounds. Bonding in any elements takes place with only the valence level electrons.

Carbon is the sixth element of periodic table and is positioned in the group IVA. Two electrons of carbon occupy the $1s^2$ orbital, these are core level electrons and are not available to form a bond. These 1s core level electrons do not generally affect the solid state properties of carbon materials, since the energy position of the 1s core levels is far from the Fermi energy compared with the valance level electrons. The other four electrons, valance electrons, occupy $2s^2$ and $2p^2$ orbitals. In the crystalline phase the valance electrons give rise to 2s, $2p_x$, $2p_y$, and $2p_z$ orbitals which are important in forming covalent bonds in carbon materials. Since the energy difference between the upper 2p energy level and the lower 2s level is smaller compared with the binding energy of the chemical bonds, the electronic wave functions for these four electrons can easily mix with each other, so changing the occupation of the 2s and three 2p atomic orbitals in order to enhance the binding energy of the C atom with its neighbouring atoms. This mixing of 2s and 2p atomic orbitals is called hybridization. In carbon, three possible hybridization occur: sp, sp^2, sp^3. This is the reason why carbon assumes in a variety structural forms such as graphite, diamond, carbon fibers, fullerenes, and carbon nanotubes.

Carbon has isomers from 0 dimension to 3 dimensions; fullerene has a zero-dimensional structure, carbon nanotubes are one-dimensional, graphene is two-dimensional and diamond is three-dimensional. Isomers of carbon are given in table 2.1.

Table 2.1 Isomers made of carbon
(Source:Dresselhaus, et al. 1993)

Dimension	0-D	1-D	2-D	3-D
Isomer	C60 Fullerene	Nanotube Carbyne	Graphite Fiber	Diamond Amorphous
Hybridization	sp^2	sp^2 (sp)	sp^2	sp^3
Density [g/cm^3]	1.72	1.2-2.0 2.68-3.13	2.26 ~2	3.515 2-3
Bond Lenghts [A^0]	1.40 (C=C) 1.46 (C-C)	1.44 (C=C)	1.42 (C=C) 1.44 (C=C)	1.54 (C-C)
Electronic Properties	Semiconductor Eg= 1.9 eV	Metal or semiconductor	Semimetal	Insulating Eg=5.47 eV

2.1.1. Diamond

There are two known three dimensional (3D) allotropes of carbon. Diamond which is one of the 3D allotrope of carbon, is reformed from graphite by applying high temperature and high pressure and it shows a sp^3 hybridization in its structure. It has a face centered cubic crystal structure and occurs from tetrahedrally bonded carbon atoms. Diamond has many uses in industry because of its excellent physical properties which are generally originated from strong covalent bonds between its atoms. The most important characteristics of diamond are its hardness, thermal conductivity, wide band gap, and high optical dispersion.

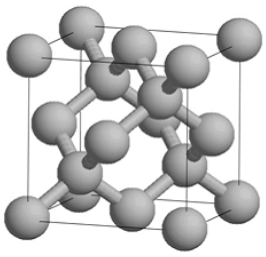

Figure 2.1. Unit cell of diamond
(Source: Stahl 2000)

2.1.2. Graphite

An other most common and 3D allotrope of carbon is graphite which is the most stable form of carbon at room temperature and atmospheric pressure (Baddour and Briens 2005). Graphite is an electrical conductor unlike diamond and it is chemically more reactive than diamond. It has a different crystal structure from diamond. It is soft and grey to black in colour. The graphite structure composes of layers of hexagonally arranged carbon atoms and within these layers, each carbon atom bonds to three coplanar neighbour atoms by strong covalent bonds but the fourth bonding in perpendicular direction is a weak van der Waals bond and as a consequence planes of graphites can be seperated easily because the interaction between two planes in graphite is very weak. Figure 2.2 shows the structure of graphite. A single atomic plane of graphite is called 2D graphite or graphene layer , and graphene is the basic structural element of also fullurenes and carbon nanotubes.

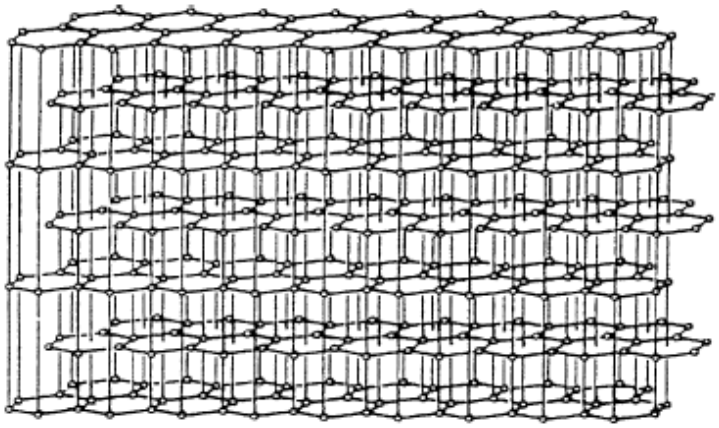

Figure 2.2. Crystalline structure of graphite
(Source : Wissler 2006)

2.1.3 Fullerene

The first discovery of fullerene, an other form of carbon, was in 1985 (Kroto, et al.1985) . Fullerene has the form of a hollow closed sphere or ellipsoid and can consist of 60, 70 or 82 carbon atoms. In the fullerene structure carbon atoms bonded to one another creates both hexagon and pentagon rings. The structure of a C_{60} molecule is called as Buckyminster fullerene and has the form of a soccer balls. It is the smallest fullerene molecule in which no two pentagons share an edge and showed in figure 2.3.

Pure fullerenes are not conductor but when they are doped with alkali metals their conductivity becomes as high as metals. They are really strong and very elastic at the same time.

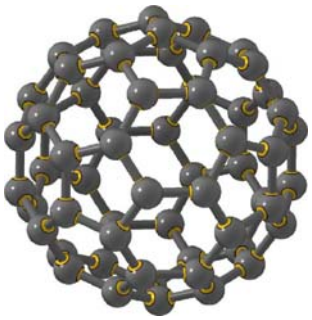

Figure 2.3. C60 Buckminsterfullerene
(Source: Wissler 2006)

Hereafter, the one dimensional carbon form which is called carbon nanotube (CNT) which is interesting with its excellent physical and chemical properties is going to be introduced, as the subject of this study.

2.2. Carbon Nanotubes

2.2.1. Discovery

By rolling a graphene sheet into a cylinder and capping both end of the cylinder with a half of fullurene molecule a carbon nanotube is formed. Harry Kroto discovered C_{60} molecule in 1985 (Kroto, et al. 1985) while experimenting a laser ablation system for the vaporization of graphite by laser beams and depositing them on a copper collector and it was the beginning of a new area in carbon material science. At 1990s arc discharge method was reported in order to make large quantities of the C_{60} molecule. In 1991, Iijima experimented this technique in order to observe fullerene and by passing large current between two graphite rods, he vaporised them and condensed them on Cu tip. When he looked at the result through an electron microscope, he noticed something unexpected, he discovered carbon nanotubes (Iijima, et al. 1991) at the negative electrode of an arc discharge. They were tiny tubes of pure carbon with a large amount of other forms of carbon. These first carbon nanotubes were like Russian

dolls, several concentric layers with caps at the end, so they were called multi-wall carbon nanotubes. TEM images of these tubes are shown in Figure 2.4.

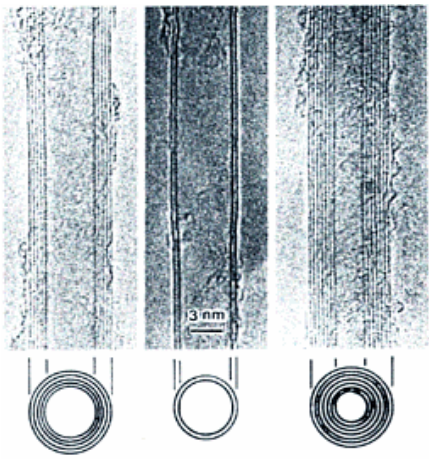

Figure 2.4. TEM images of MWNTs observed by Sumio Iijima
(Source: Iijima 1991)

Only two years later, in 1993, single-wall carbon nanotubes could be grown using Co metal catalysts by arc discharge method (Iijima, et al. 1993).

2.2.2 Types of Carbon Nanotubes

Type of carbon nanotube is determined by the number of the concentric graphene layers. Carbon nanotubes are categorized as single wall carbon nanotubes and multi wall carbon nanotubes. If carbon nanotube contains one graphene layer, it is named single wall nanotube (SWNT); whereas if it contains two or more concentric layer, it is called multi wall carbon nanotube (MWNT).

2.2.2.1 Single Wall Carbon Nanotube

A single-wall carbon nanotube (SWNT) is defined by a graphene sheet rolled into a cylindrical shape with a diameter of about 0.4-10 nm and lengths extending up to several microns. The shape of a SWNT is depicted in figure 2.5. If we ignore two ends of carbon nanotube and focus on the large aspect ratio of the tube, carbon nanotubes

can be considered as one-dimensional nanostructures with axial symmetry and they have excellent properties because of this symmetry (Baddour, et al. 2005).

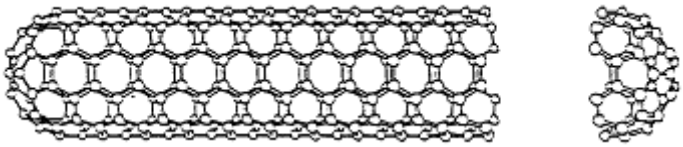

Figure 2.5. An illustration of a SWNT
(Source :Dresselhaus 1998)

2.2.2.2. Multi-Wall Carbon Nanotube

The second type consists of tubes made of more than one concentric graphene cylinders coaxially arranged around a central hollow with a constant interlayer spacing which is nearly equal to 0.34 nm (Dresselhaus, et al. 2001), graphite layer spacing, and called multi-shell or multi-wall carbon nanotubes (MWNT) and it is depicted in figure 2.6. MWNTs consist in 2 to 30 concentric graphene, diameters of which range from 2.5 to 100 nm. MWNTs are stronger than SWNTs , but they have more defects than SWNTs (Dai 2002).

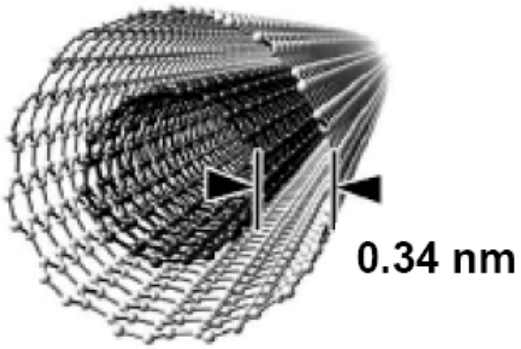

Figure 2.6. An illustration of a MWNT
(Source : Iijima 1999)

2.2.3. Classification of Carbon Nanotubes

A single-wall carbon nanotube can be found in three different configurations with respect to the orientation of the six-membered carbon ring (hexagon) in the honeycomb lattice relative to the axis of the nanotube. These configurations are armchair carbon nanotube, zigzag carbon nanotube and chiral carbon nanotube. In Figure 2.7 the formations of each of three nanotubes are depicted.

The basic shape of the carbon nanotube wall is a cylinder, and the terminations of carbon nanotubes consist of a hemisphere of fullerene caps or end caps. However, as it is shown in Figure 2.7, the direction of six-membered ring in the graphene lattice relative to the axis of the nanotube can be taken almost arbitrarily, without any distortion of the hexagons except for the distortion due to the curvature of carbon nanotubes. This is why carbon nanotubes occur in many different chirallities.

Carbon nanotube can be also classified into two groups; achiral and chiral nanotubes. An achiral carbon nanotube is a carbon nanotube whose mirror image has an identical structure to the original one. There two types of achiral carbon nanotubes and these are armchair and zigzag nanotubes. Chiral nanotubes show a spiral symmetry whose mirror image cannot be superposed on to the original one.

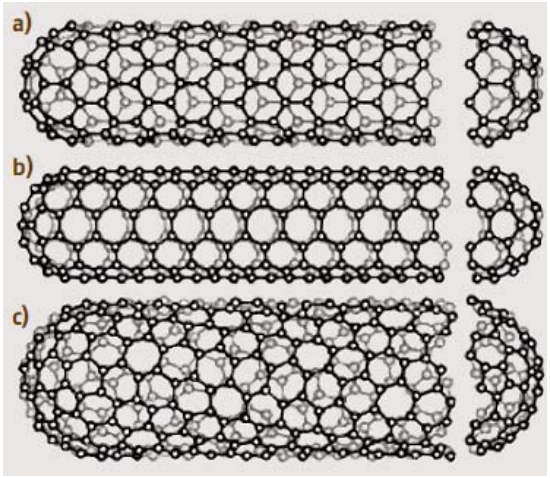

Figure 2.7. Classification of CNTs a) Zig-zag b) Arm-chair c) Chiral CNTs
(Source : Dresselhaus, et al. 1995)

The atomic structure and type of a carbon nanotube is controlled by its chiral vector (C_h= n$\hat{a}_1$+m$\hat{a}_2$) and its chiral angle (θ) (Reich, et al. 2004). These (n, m) values are pair of integers which specify the chiral vector and $\hat{a}_1$, $\hat{a}_2$ are unit vectors of the hexagonal honeycomb lattice of the graphene sheet. The chiral angle (θ) gives information about orientations of CNTs. The chiral angle (θ) , as shown in Figure 2.8, is defined as the angle between the chiral vector C_h and $\hat{a}_1$, with values of θ in the range of 0 ≤θ≤ 30 (Rotkin and Subramoney 2005).

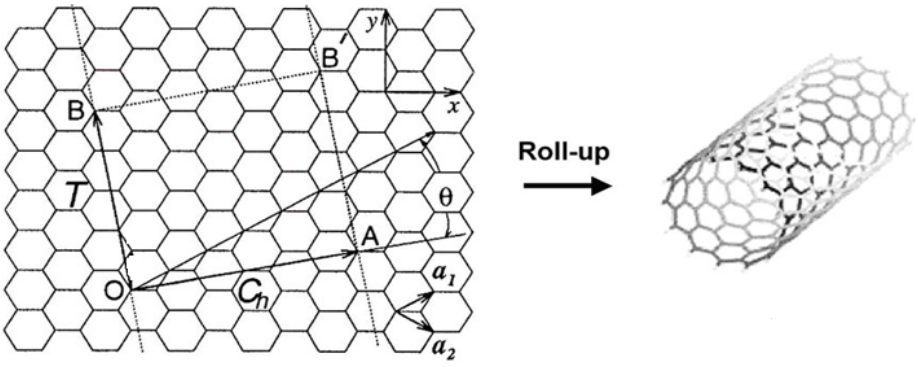

Figure 2.8. An illustration of rolling graphene into a tube
(Source: Saito, et al. 1998)

While n=m corresponds armchair type CNT at θ=0^o, m=0 corresponds zigzag type CNT at θ=30^0, and if n≠m the tube is chiral and chiral angle is between 0^0 and 30^0 (Belin and Epron 2005). Chirality defines also the electrical properties of carbon nanotube. If (2n+m) or equivalently (n-m) is a multiple of 3, a metallic nanotube occurs. The armchair nanotubes denoted by (n,n) are always metallic if n is a multiple of 3, and the zigzag nanotubes (n,0) also are metallic. In figure 2.9 which carbon nanotubes are metallic and which are semiconducting is shown. The encircled dots are the metallic nanotubes, the small dots are the semiconducting nanotubes.

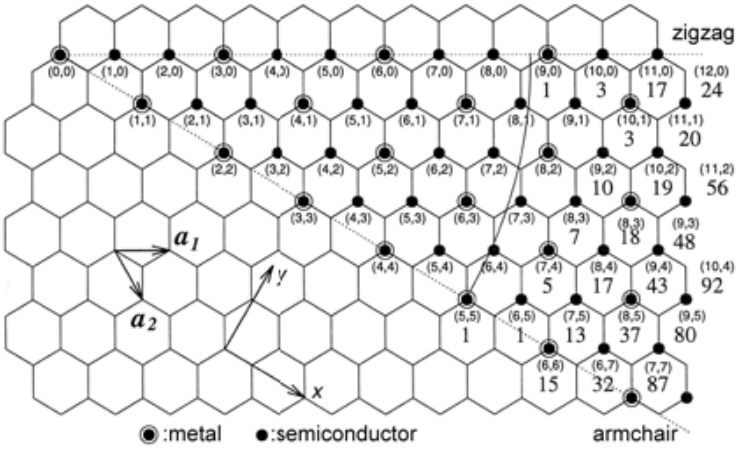

Figure 2.9. Possible vector specified by the pairs of integers (n,m)for general CNTs (Source: Dresselhaus, et al. 1993)

2.3. Carbon Nanotube Synthesis Methods

There are several methods to synthesize CNT, the most common techniques are discharge (Journet, et al. 1997), laser ablation (Thess, et al.1996), and chemical vapor deposition (CVD) (Niu, et al. 2006) methods. Arc discharge method is the method in which first CNT growth method, but in this method CNTs are found together with large concentration of amorphous carbon and CNTs are not aligned. Laser ablation method is the second method and it can provide arrays of ordered CNTs. The last technique is CVD technique which is appropriate for scaling-up. While arc discharge and laser ablation methods require a solid target and very high temperatures to evaporate it, CVD method can be used at lower temperature, and the CNTs obtained from both with arc-discharge and laser ablation methods are tangled and thus purification is not evident for these methods. All of these three methods have some advantages and disadvantages, each technique will be shortly explained below.

2.3.1. Arc-Discharge Method

The first carbon nanotubes are produced with arc discharge method (Iijima 1991). This method has been used for synthesis of single-wall carbon nanotubes, multi-wall nanotubes, and ropes of single-wall nanotubes (Journet, et al. 1997). This method is the process of CNT growth on carbon (graphite) electrodes by applying direct current

(DC) in an inert gas such as argon or helium (Popov 2004). Figure 2.10 is a schematic illustration of the arc-discharge setup.

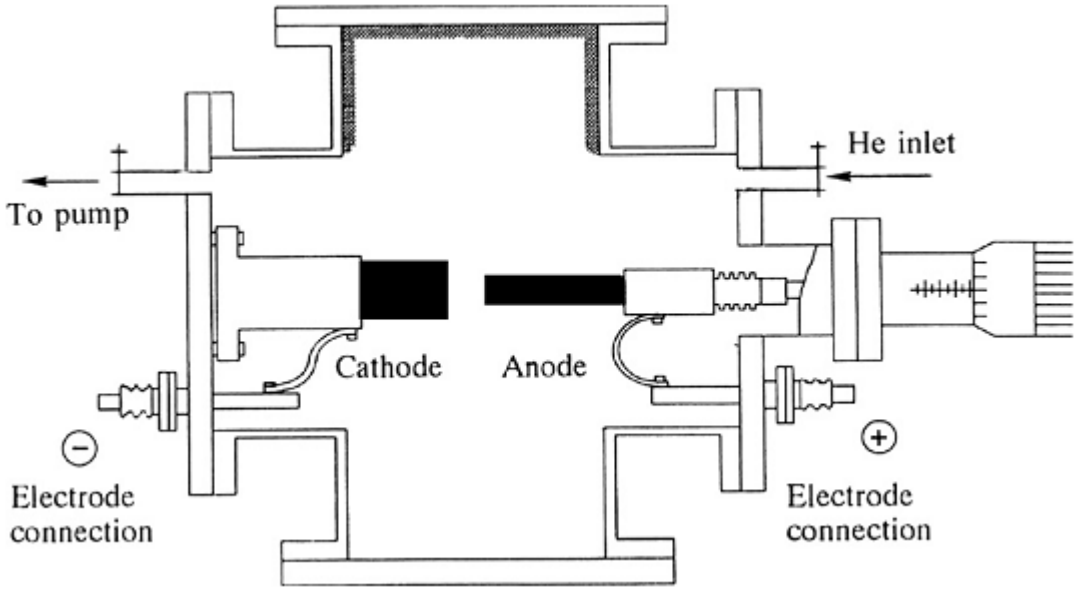

Figure 2.10. Cross sectional view of a arc generator
(Source: Harris 2007)

In this method, there are two high-purity graphite electrodes of 5-20 mm diameter separated by 1 mm. A voltage of 20-25 V is applied across the electrodes and a dc electric current of 50-120 A flows between the electrodes. When applying current, temperature reaches to about 4000^{o}C, anode vaporises and condenses on the cathode surface, so the length of anode decreases with the formation of carbon nanotubes. During the process both electrodes are cooled with water, and the arc is generally operated in He atmosphere at low pressure between 50-700 mbar. By the arc discharge method carbon nanotube synthesis can be done with or without catalyst in order to produce multi-wall carbon nanotubes and single-wall carbon nanotubes, respectively (Journet and Bernier 1998).

For multi-wall carbon nanotube production, there is no catalyst need, and nanotubes are found in bundles in the inner region of the cathode deposit and are roughly aligned in the direction of electric field (Ebbesen, et al. 1993, Seraphin, et al. 1993). Using this method Iijima produced first multi-wall carbon nanotube in 1991, and these nanotubes had 2 to 50 walls. However, many by products also occur at this method such as fullerenes, amorphous carbon, graphite sheets (Baddour 2005). By heating the as grown material in oxygen environment, graphitic particles can be

oxidized and purification is provided, but oxidation also removes an substantial amount of nanotubes.

When one of the graphite electrodes (anode) contains a transition metal catalyst particles such as Fe, Co, Ni, single wall carbon nanotubes can be synthesized using arc discharge method. First single-wall carbon nanotube synthesis by arc discharge method was reported in 1993 by Iijima and Ichihashi, and the used catalyst was Fe in their study. In the same year Bethune et al. also syntesized single- wall carbon nanotubes with this method, but using Co as a catalyst. There are a lot of study about single-wall carbon nanotube synthesis but the results always change, it can be said that experimental conditions and catalyst species effects the results .

As a conclusion, arc discharge is the most common and simplest method to produce carbon nanotubes, but it require a purification and the purification is the main disadventage of this method, since during this process carbon nanotubes might be damaged.

2.3.2. The Laser Ablation Method

The first carbon nanotube synthesis by laser ablation method was reported by Guo (Guo, et al. 1995). This method utilizes an intense laser pulse (Yudasaka, et al. 1999) or a continous laser (Maser, et al. 1998) to ablate a Co-Ni/graphite composite target. The target is placed in a tube furnace heated to 1200^{o}C. When this target vaporises, a cloud of C, C_2, C_3 and catalyst vapors occur, then cloud condenses, and the small amount of carbon species come together to form a larger one. The vaporized catalysts prevent the closing of these carbon molecules into cage structure, so the growth process is finished with the formation of a single-wall carbon nanotube (Scott, et al. 2001, Baddour and Briens 2005). During the laser ablation, an inert gas (generally helium or argon) flow take place in the growth chamber and provides grown carbon nanotubes to collect on a water-colded cupper collector as shown in figure 2.11. Laser has a very high energy density so this method is appropriate to evaporate materials that have high evaporation temperature (Ando et al. 1994). With increasing laser power, target temperature increases, hence the yield of carbon nanotubes improves.

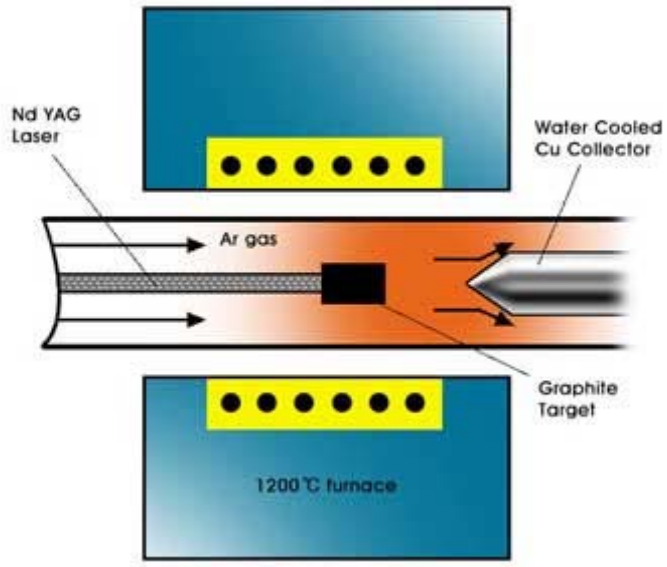

Figure 2.11. Schematic illustration of a laser ablation apparatus
(Source : Daenen, et al. 2003)

Relatively high purity single-wall carbon nanotube synthesis is the main advantage of laser ablation method. With this technique, multi-wall carbon nanotube synthesis has not been reported yet. On the other hand, scale-up is not possible with this method because of very high temperature and capital cost need.

2.3.3. Chemical Vapor Deposition Method

The general nanotube growth mechanism in a chemical vapor deposition process through the dissociation of hydrocarbon molecules over the transition metal nanoparticles and dissolution and saturation of carbon atoms in these nanoparticles. CVD method has been used first for the production of carbon filaments more than 4 decades ago (Walker, et al. 1959), however, it was utilized to grow multi-wall carbon nanotubes till 1993 (Yacaman, et al. 1993). Some different CVD techniques have been developed for carbon nanotube growth such as plasma enhanced CVD, thermal CVD, alcahol catalytic CVD, laser assisted CVD and aero-gel supported CVD. Thermal CVD method will be explained below in details.

Carbon nanotube growth includes two main step; the first one is the catalyst preparation and the other one is the nanotube growth on this catalyst. In order to synthesis nanocatalyst particles, a thin film layer can be used by annealing or a catalyst can be synhesized by some chemical methods. At the first step, prepared catalyst

sample is placed in a quartz tube which is in a furnace and the temperature is set to a desired point. During the increase of the temperature to the set point, an inert gas flow takes place through the tube to prevent the oxidation of samples. When the furnace reaches to the desired temperature a preannealing can be done with H_2 to reduce catalyst nano particles from oxide form to metal form. The other step is sending hydocarbon gas to the system as a carbon precursor. Generally used hydrocarbon gases are CH_4, C_2H_4, C_2H_2, C_6H_6 for carbon nanotube growth (Cui, et al. 2003). During growth process, hydrocarbon gas decomposes and carbon deposits onto the catalyst. Carbon has a low solubility in these metals at high temperature and therefore the carbon precipitates to form cabon nanotubes.

The key parameters in nanotube growth by CVD are the catalyst system, temperature, composition and the flow rate of the carrier and hydrocarbon gases (Biris, et al. 2006). The particle structure and composition also are very important parameters to explain the differences observed between the nanotubes morphologies (Loiseau, et al. 2003). In CVD method Fe, Co, Ni transition metals or their alloys are used as catalyst to synthesize carbon nanotubes. As support, inorganic porous materials such as silica (SiO_2), alumina (Al_2O_3), zeolites and magnesium oxide (MgO) are generally used (Liu, et al. 2004).

CVD is the most preferred method to produce carbon nanotubes, because this method is performed at low temperature compared with the other methods (Reich et al. 2004). The other reason is this method allows to control the diameter of CNTs by controlling catalyst nanoparticles size (Weifeng, et al. 2003). At the same time it is easy to perform CVD process. An other reason is that it is suitable method for large scale production (Yamacan, et al. 1993, Weifeng, et al. 2003). The schematic illustration of CVD system is depicted in Figure 2.12.

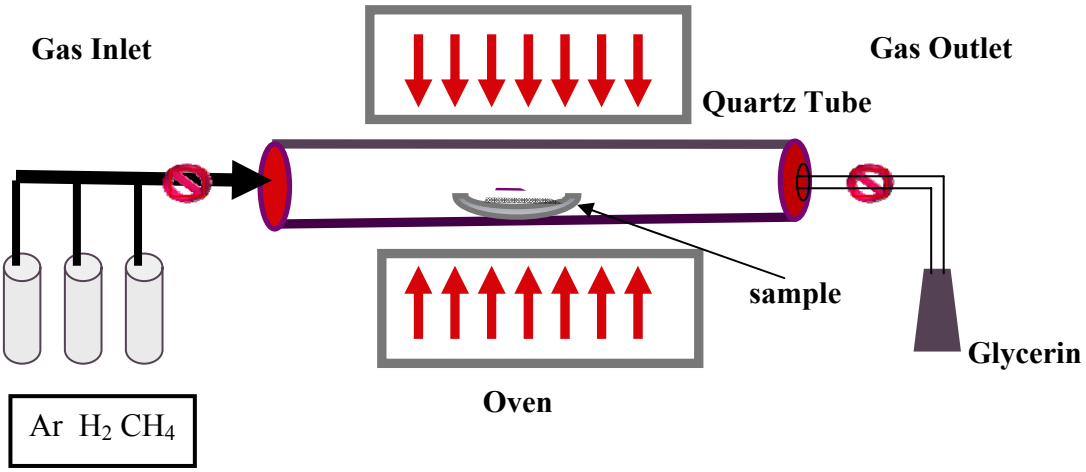

Figure 2.12. A schematic illustration of a CVD System

There are two types of CNT growth mechanism. The first one is the base growth in which the metal catalyst particle stay at the end of the tube. The other growth type is the tip growth in which the metal catalyst particle might remove from the surface and moves at the top of the growing carbon nanotube (Dupuis 2005). The interaction between catalyst particle and support is stronger at base growth mechanism than tip growth mechanism so catalyst particle remains attached to the support (Dupuis 2005). The types of growth mechanisms are given at Figure 2.13.

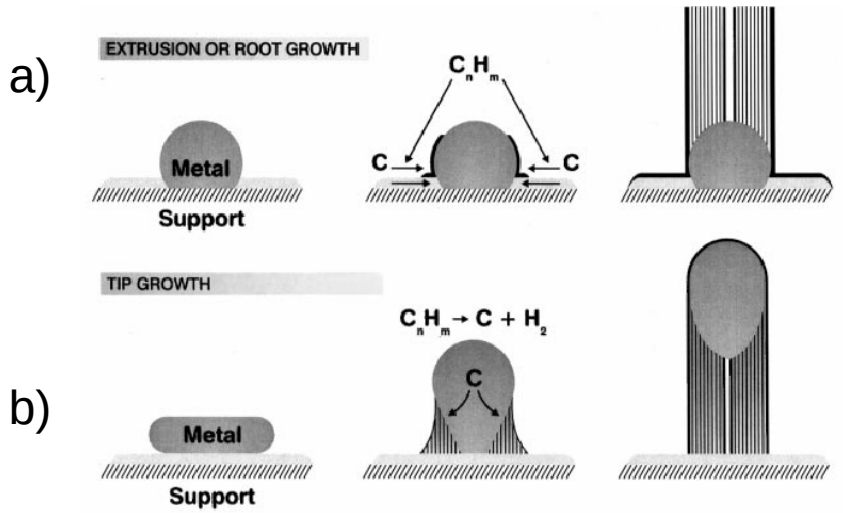

Figure 2.13. Schematic illustrations of carbon nanotube growth mechanisms a) Base or root growth b) Tip growth (Source: S.B.Sinnot, et al. 1999)

CHAPTER 3

CATALYST USED FOR CNT GROWTH

3.1. Catalyst

As explained in the previous chapter, most of the CNT synthesis methods require catalyst particles. A catalyst is described as a susbtance that increases the rate at which a chemical reaction approaches equilibrium without itself becoming permanently involved in the reaction (Richardson 1989). But the main role of catalyst in CNT growth is to decompose hydrocarbon molecules (Dupuis 2005).

The catalyst material is one of the most important key parameters, and determines the morphology, type (SWNT or MWNT), diameter and also growth mechanism in the production of CNTs. CNT formation is affected by method of catalyst preparation (Bonadian, et al. 2006), the nature and pore size of the support (Qingwen, et al. 2002), the nature of the metal (Ago, et al. 2006), the quantity of active catalyst particles and size and size distribution of the active component.

3.1.1 Literature Search

In this section, number of studies about CNT growth on catalysts synthesized by chemical methods are given in table 3.1. An extensive literature search was done in order to find an ideal catalyst for CNT growth.

Table 3.1 List of some studies on CNT growth

Reference	Catalyst Preparation Method	Experimental Details	Results
Kong, et al. 1998	Method: Impregnation Materials: Fumed alumina, $Fe(NO_3)_3.9H_2O$, Methanol	Catalyst mass:10mg T:1000 C Methane flow: 6150sccm P:1.25atm Time: 10 min	They obtain abundant individual SWNTs in the diameter range of 1.3-5.4 nm for Fe_2O_3/ alumina catalyst. They obtained only boundles of SWNTs for silica supported catalyst.
Cassel, et al. 1999	Method: Impregnation Prepared catalysts: $Fe_2(SO_4)_3/Al_2O_3$, $Fe(NO_3)_3/Al_2O_3$, Fe-Mo/Al_2O_3 and Fe-Ru/Al_2O_3 Molar ratio: Fe:Al_2O_3= 1:16 For bimetallic (Fe/Mo and Fe/Ru) catalysts molar ratios:	Catalyst mass: 100 mg, Quartz tube diameter: 2.54 cm Temperature: 900 ^oC CH4: 6000sccm Growth time: 2-45 min. For heating and cooling processes Ar gas was used.	High quality and yield of SWNTs were obtained over Fe-Mo/ Al_2O_3 and Fe-Mo/SiO_2 catalsyts. It was attributed to dispersion, high surface area and metal support interraction.

(cont. on next page)

Table 3.1 (cont.)

	Fe: X(Mo or Ru): Al_2O_3= 1:0.17:16 For Al2O3-SiO2 hybrid support material molar ratio: Fe: Mo: SiO2: Al2O3=1:0.17:16:16 Calcination temperature: 500 ^oC		
Qingwen, et al. 2002	Method: Impregnation Active Metals: FeO, CoO and NiO Supports: SiO_2,ZrO_2,CaO. Al_2O_3, or MgO All the supported catalysts were prepared by sonicating the support material in aques nitrate solution of Fe, Co or Ni at the desired concentration (10-15 %) for several minutes. The resultant mixture was	Catalyst mass: 1g Temperature: 850 ^oC Ar flow: 250 sccm Time :30 min Purification was done 4 M HCl for several hours for MgO support. Ar/CH_4 =250 ml/min/60 ml/min. FeO content from 5 to 50 %.	When Fe was used MWNTs were observed on SiO_2, ZrO_2, and CaO supported catalysts while SWNTs were observed on Al_2O_3 and MgO supported catalysts. The quality of as grown SWNTs on MgO supports is stable for all Fe, Ni and Co metals. FeO/MgO was favorouble for SWNT. The obtained purity after purification is higher than 90%, and yield was around 10 %. Optimal growth temperature was found in the range

(cont. on next page)

Table 3.1 (cont.)

	then dried at 115 ^{o}C for at least 5 h and then ground to fine powder.		of 700-950 ^{o}C. Yield increased significantly by Mo addition.
Liu, et al. 2003	Method: Impegnation Materials: $Fe(NO_3)_3.9H_2O$, Mo solution, MgO powder, DI water Weigth ratio: Fe:Mo:MgO=1:0.1:11	Carbon precursor: C_2H_2 Catalyst mass: 300mg Temperature: 800-950 ^{o}C Ar flow:2000 sccm Time: 20min	High quality SWNTs with few defects and very small amount of amorphous carbon coating have been produced. It was observed that C_2H_2 is more reactive than CH_4 at the same reaction temperature.
Liu, et al. 2005	Method: Impregnation Materials: $Fe(NO_3)_3.9H_2O$, $Co(NO_3)2.6H_2O$, MgO, DI water Molar ratio: Fe:Co = 1.4:1.0	Temperature: 1000 ^{o}C CH_4 flow: 1000sccm Time: 30min	DWNTs were obtained in diameter is about 0.5-5 nm. They are pure and almost no amorphous carbon formation.
Yu, et al. 2006	Method: Impregnation	Dilutent gas: H_2: methane =	Effect of N_2 and Ar atmosphere on CNT growth

(cont. on next page)

Table 3.1 (cont.)

	Materials: $Fe(NO_3)_3.9H_2O$, $(NH_4)_6Mo_7O_{24}$, MgO powder, BET 27.4 m^2/g. DI water Weight ratio: 1:10, Molar ratio: Fe/Mo=1:3.5 (Fe to Mo)	10:1:1 Temperature: 900 ^oC Time: 30 min	was investigated as a diluting gas. In argon atmosphere SWCNTs were synthesized. It was observed that nitrogen is not inert in CNT growth by the CVD method.
Ago, et al. 2006	Method: Impregnation Materials: $Fe(NO_3)_3.9H_2O$, $Co(NO_3)_3.6H_2O$, $Ni(NO_3)_2.6H_2O$, $MoO_2(acac_2)$, MgO powder, Methanol Metal loading : 1wt%	Catalyst mass:1g Temperature:800 ^oC Ar flow: 350 ml/min CH_4 flow: 350 ccm Growth time:1 hour Preannealing time: 1 h Preannealing temperature : 800 ^oC	Catalytic activity decreased with the species used in order to Fe-Mo>Fe>Co>Ni. They obtain SWCNTs and DWCNTs. A small amount of water vapor assist the growth of SWCNTs.
Kang, et al. 2006	Method: Impregnation Materials: $Fe(NO_3)_3.9H_2O$,	Catalyst mass: 20 mg, Tube length: 850mm, diameter: 50	They obtained 1.6-2.4nm SWNTs. The nanotubes composed of about %95 SWNT

(cont. on next page)

Table 3.1 (cont.)

	$(NH_4)_6Mo_7O_{24}.4H_2O$, MgO powder Molar ratio: Fe:Mo=9:1 Total metal loading: 4wt% Reduction at 500 ^oC for 10 hour under 40sccm H_2 gas flow.	mm Carbon source: CH_4 Carrier gas: H_2 Reaction temperature: 800,850, 900,950, and 1000 ^oC Time: 30 min	and %5 DWNT at 800 ^oC growth temperature. They observed that with increasing temperature the number of DWNTs increases.
Bonadian, et al. 2006	Method-1: Impregnation Materials: 8.08 g. $Fe(NO_3)_3.9H_2O$, 0.205 g. $(NH_4)_5Mo_7O_{24}.4H_2O$, 12.3 g. commercial magnesia, 200 ml of DI water Method-2: combustion Materials: $Mg(NO_3)_2.6H_2O$, $(NH_3)_6Mo_7O_{24}.4H_2O$, $Fe(NO_3)_3.9H_2O$, Citric acid, DI water	Temperature: 950 ^oC Time: 30 min. Ar: 100 sccm CH4: 25,19,12,6,3 sccm	The Fe-Mo/MgO catalyst produced better results regarding number of CNT and their diameters under Ar/ NG atmospheres than under H_2/NG atmospheres, resulted in the formation of thinner and cleaner CNT. SWNTs and DWNTs formed. CNTs with diameter between 0.6 and 1.8 nm. were obtained for 25 sccm CH_4. The diameter of MWNTs were between 40 and

(cont. on next page)

Table 3.1 (cont.)

	Molar Ratio: Fe/MgO/Mo= 1:10:12		80 nm when the catalyst is produced with combustion method.
Chai, et al. 2006	Method: Impregnation Materials: $Co(NO_3)_2.6H_2O$ Loading amount: 10 wt.% $Cu(NO_3)_2.3H_2O$ $Fe(NO_3)_2.9H_2O$ $(NH_4)_6Mo_7O_{24}.4H_2O$ $Ni(NO_3)_2.6H2O$, DI water Supported materials: SiO_2, zeolite, Al_2O_3, ceria, TiO_2, MgO, CaO	Pressure: atmospheric pressure Methane/Nitrogen: 1/1 Catalyst mass: 200 mg Temperature : 550 ^oC or 700 ^oC	At 550 ^oC the carbon capacity over the supported CoO catalyst was found to decrease in the order of silica> zeolite> alumina> ceria> titania> magnesia> calcium oxide. It was observed that the carbon capacity decreased, following the order of alumina> ceria> zeolite> silica> titania> calcium oxide> magnesia at 700 ^oC. The average diameter calculated was 10.7 nm. MoO increased the carbon capasity and the selectivity of CoO/Al_2O_3.
Jodin, et al. 2006	Catalyst A: Fe and Mo nanoparticles deposited on silicon substrates	Carbon precursor: CH_4 Temperature: 800-1000 ^oC	MWNTs formation was observed on catalsyt A, no SWNT

(cont. on next page)

Table 3.1 (cont.)

	Catalyst B: Fe-Mo/ Fumed alumina catalyst Catalsyt C: Fe-Mo/Al_20_3	Time: 10 min Quartz tube diameter: 4 cm, Ar: 1000 sccm	Catalyst B gave SWNT and DWNT. Catalyst C gave SWNT of different sizes and narrow diameter compared to SWNTs obtained from catalyst B.
Yoshihara, et al. 2007	Method: Impregnation Materials: $Fe(NO_3)_3.9H_2O$, $MoO_2(acac_2)$, MgO powder, Methyl alcohol Fe:Mo atomic ratio : 94:6 Total metal loading: 1wt%	No details given.	With increasing CVD temperature from 800^{o}C to 900^{o}C, the carbon yield decreased from 19 wt% to 13 wt%. The precise control of water concentration and temperature is important for effective SWNT and DWNT .
Wen, et al. 2007	Method: Impregnation Materials: $Fe(NO_3)_3.9H_2O$ $(NH_4)_6Mo_7O_{24.}$ $4H_2O$ MgO powder, $SiO_{2,}$ Al_2O_3	T: 900 ^{o}C 5% H_2 and 95% CH_4, with and without a CO_2 mixture (10% CO_2 + 90% Ar, premixed).	The synthesis in the absence of CO_2 gave SWNT products that contained some very short tubes and relatively more broken carbon sheets. The presence of CO_2 caused to decrease in size

(cont. on next page)

Table 3.1 (cont.)

	The catalyst molar ratio: Fe:Mo:support=0.02:0.0013:1 .	The concentration of CO_2 was controlled to 0.1-2.0% in the reactant gas (CH_4) Growth time: 15 min.	of the MgO support and increase specific surface area of the catalyst, but too much CO_2 will also react with the SWNTs and decreased the yield. CO_2 was proved operative on the catalysts using a MgO support but not on the catalysts using a Al_2O_3 or SiO_2 support.
Kathyayini, et al. 2008	Method: Dry impregnation Materials: $Al(OH)_3$: 19g $Fe(NO_3)_3.9H_2O$: 3.6 g, $Ni(NO_3)_2.6H_2O$, $Co(NO_3)_2.6H_2O$: 2.5 g Molybdenum acetilacetonate	Temperature: 700 ^oC Catalyst mass: 1g Diluting gas: N_2 N_2 flow: 300 sccm (10min) C_2H_2 flow: 30 sccm (60min)	They made trimetalic catalysts (combinations of Fe,Co,Mo,Ni) but as grown CNTs contained higher percentage of amorphous carbon. For $Al(OH)_3$ support, bimetalic catalysts generally generated good quantity of CNT with high density and precence of Mo decreased the activity and promoted the amorphous carbon formation.

(cont. on next page)

Table 3.1 (cont.)

			They obtained MWCNTs.
Biris, et al. 2008	Method: Impregnation Materials: $Fe(NO_3)_3.9H_2O$, $(NH_4)_6Mo_7O_{24}.4H_2O$, MgO powder, DI water Weight ratio: Fe:Mo:MgO=1:0.1:12	They use RFCVD Catalyst mass: 100 mg Temperature: 850^oC Frequency: 350kHz Time:30 min	The carbon deposit and the size of nanotube boundles increased with hydrogen level. Hidrogen gas source was used for etching the amorphous carbon.
Liu, et al. 2009	Method: Impregnation Materials: Ammonium iron citrate $(NH_4)_6Mo_7O_{24}$ MgO powder For MoO_3 conditioning catalysts, $(NH_4)_6Mo_7O_{24}.,4H_2O$ (200 mg)	Mass: 50g The mixture of CH_4 and Ar (volume ratio: 1/1) as carbon source was fed at 200 sccm) Time: 10 min Temperature: 875 ^oC	In the samples obtained with and without MoO_3, the I_D/I_G values were about 0.200 and 0.400, respectively. The higher ID/IG value without MoO_3 means that the relative purity and crystallinity of the products were lower than those obtained with MoO_3. Fe–Mo/MgO catalyst itself showed a higher production yield of CNTs than the Fe/MgO catalyst.

(cont. on next page)

Table 3.1 (cont.)

Su, et al. 2000	Method: Sol-gel, supercritical drying. Materials: Aluminum tri-sec-butoxide, Ethanol $Fe(SO_4)_3.4H_2O$, $MoO_2(acac_2)$, Nitricacid Ammonium hydroxide, Molar ratio: Mo: Fe: Al=0.16:1:16	Catalyst mass:50mg, Temperature: 850 ^oC to 1000 ^oC Before growth reduction with 100 sccm H_2 flow for 30min CH_4 flow:1000 sccm Growth time: 60 min. Purification with 3 M HNO for 4 h.	They obtained high-quality SWNTs. This was attributed to high surface area of support and metal-support interraction. High dispersion leading to SWNT formation. Improvements in SWNT yield was attributed to strong interractions between the aerogel support and the catalyst as well as the high surface are of the support.
Ning, et al. 2002	Method: Sol-gel Materials: Citric acid, $Mg(NO_3)_2$, $6H_2O$, $Co(NO_3)_2.6H_2O$, DI water, Mo powder	T: 1000 ^oC CH_4: 1000 sccm H_2: 30sccm Time: 30 min	Pores and channels might form due the high temperature or the force of growing tubes. They were parallel to each other because of the preferred crystallographic orientation. Anyway, aligned bundled carbon nanotubes grow out of these parallel channels.
Mehn, et al. 2004	Methos: Sol-gel	Condition A:	The best results was obtained by using

(cont. on next page)

Table 3.1 (cont.)

	Materials: Aluminum tri-sec-butoxide, Butanediol, 2-butanol, 1,3-butanediol, $Fe_2(SO_4)_3.5H_2O$, $Fe(NO_3)_3.9H_2O$, $Fe(acac)_2$, $(NH_4)_6Mo_7O_{24}.4H_2O$, MoO2(acac)2	Reduction with 200 sccm H_2 for 30 min at 900 ^oC Growth tme: 30 min CH_4: 1000 sccm Temperature: 900 ^oC Condition B: Reduction with 500 sccm H_2 and 500 sccm CH_4 for 6 min at room temperature Growth time: 10 min, H_2: 500 sccm CH_4: 500 sccm, Temperature: 950 ^oC	$Fe(NO_3)_3.9H_2O$ in methanolic as well as in ethanolic solutions. Absence of molybdenum led to decreased activity and the formation metal particles in the size range of 4–10 nm. Decreasing Fe/Al ratio from 1 to 0.5 in the catalyst results in a small decrease of the carbon yield but results also in the formation of a more uniform product. Conditions B were more favorable for SWNT formation. At elevated temperatures, amorphous carbon covering the tubes was also be observed besides MWNTs.
Tran, et al. 2006	Method: Sol-gel	Catalyst mass: 0.5g	TEM results showed that all catalysts produce

(cont. on next page)

Table 3.1 (cont.)

	Materials: $Fe(acac)_3$, $Fe(NO_3)_3$, $Co(acac)_2$, $Co(OAc)_2$, DI water, Ammonia, The total amount of metal in each catalyst has been kept constant at $0.7*10^3$ mol of metal per gram of catalyst	Temp. :700 ^oC Time:15 min. C_2H_4: 0,223mmol.s^{-1} He: 0,521 mmol s^{-1}	not only carbon nanotubes but also amorphous carbon. The catalytic activity of the metal species towards a carbon deposit is found to decrease in the order of Co > Fe > Fe–Co. Fe/Al_2O_3 catalyst synthesized with $Fe(NO_3)_3$ has a better activity and selectivity than synthesized with $Fe(acac)_3$.
Rashidi, et al. 2007	Method: Sol-gel Materials: $Co(NO_3)_2.6H_2O$ $Mg(NO_3)_2.6H_2O$ $(NH4)_6Mo_7O_{24}.4H_2O$ Molar ratios: Co:Mo:MgO = 0.5:0.25:10 Citric acid, tartaric acid, EDTA,	Reduction under 200 sccm H_2 flow rate at 850 ^oC for 1 h. Growth temperature:1000 ^oC CH_4 flow:50 sccm H_2 flow: 200 sccm Growth time: 40 min. Purification with 4 M. HCl	The organic additives increased the BET surface area of the catalysts in order of tartari acid< citric acid< EDTA < sorbitol. The yield and quality of CNTs strongly depend on the dispersion of the cobalt-molybdenum catalyst on MgO. The size of CNTs were in the range 2-5 nm.

(cont. on next page)

Table 3.1 (cont.)

	sorbitol		
Xuan-ke, et al. 2008	Method: Sol-gel Materials: $Al(NO_3)_3.9H_2O$, $Fe(SO4)_3.6H_2O$, Ethanol Molar ratio: 30:1 Temp: Room temp., Time: 24h Supercrytical drying conditions: 250 ^oC and 7.5 MPa for 0.5 h.	Catalyst mass: 1g Temperature: 900 ^oC CH_4/H_2 mixture or $CH_4/H_2/H_2O$ mixture took place on growth. H_2: 400 sccm CH_4: 600 sccm Time:30min	SWNTs prepared under $CH_4/H_2/H_2O$ gases had higher purity and the boundaries between SWNT bundles were easily discernible than the SWNTs prepared from CH_4/H_2 alone.
Li, et al. 2004	Method: Combustion Route Materials: Citric acid, Polyethylene glycol 200, $(NH_4)_6Mo_7O_{24}.4H_2O$, $Mg(NO_3)_2.6H_2O$, $Fe(NO_3)_2.9H_2O$ Molar ratios: Fe:Mo:MgO=1:0.05:13 (catalyst A)	Quartz tube diameter: 4mm, lenght: 1000mm Temperature: 1000 ^oC Catalyst mass: 200 mg N_2: 400 sccm (for 5 min) Subsequently, a mixture of CH_4=75 sccm, H_2= 300 sccm or	Catalyst A,B,C reveal no difference between the carbon fibers produced in CH_4/H_2 or CH_4/N_2 atmospehere. Average CNT diameters were 0.80 nm for catalyst A, 0.90 nm for catalyst B, and 1.05nm for catalyst C. It was observed that the diameters increased

(cont. on next page)

Table 3.1 (cont.)

	Fe:Mo:MgO=1:0.1:13 (catalyst B) Fe:Mo:MgO=2:0.1:13 (catalyst C)	CH_4= 50 sccm N_2=300 sccm Time: 30 min	with increasing Fe-Mo/MgO ratio.
Liu, et al. 2005	Method: Combustion Route Materials: $Mg(NO_3)_2.6H_2O$, Citric acid, H_2O, $Fe(NO_3)3.9H_2O$ $(NH4)_6Mo_7O_{24}.4H_2O$ Atomic ratio Mo:Fe=1:10	Ar: 200sccm 200 sccm of Ar stream was introduced into the reactor through ethanol Time: 30min	The diameters of CNTs were in the range of 1.42 and 1.48 nm. It was found that the samples had little nanotube defects, amorphous carbon and nanocrystalline impurities.
Li, et al. 2005	Method: Combustion Route Combustion additive: Polyethylene glycol 200 (PEG 200) Mg(NO3)2.6H2O,	Catalsyt mass: 50mg Quartz tube diameter:50mm, length: 1000mm, T: 1000 ^oC	Fe-Mo/MgO gave higher yield of MWNT compared to, Mo/MgO, Ni/MgO and Fe/Mo/MgO catalysts. The purity was above 97 %.

(cont. on next page)

Table 3.1 (cont.)

	(NH3)6Mo7O24.4H2O, Ni(NO3)2.6H2O Molar ratio: Mg/Mo/Ni/PEG200= 1.0/1.2/0.1/1.0 Combusition at 650 ^{o}C for 10 min.	CH4: 900 sccm, H_2: 100 sccm Investigated growth times: 10, 30, 45, 60 and 120min. For both heating and cooling N_2 gas was used.	
Niu, et al. 2006	Method: Combustion Route. Materials: $Mg(NO_3)_2.6H_2O$; $NH_4)_5Mo_7O_{24}$. $4H_2O$, $C_6H_8O_7$. H_2O(citric acid), $Fe(NO_3)_3.9H_2O$, DI water Molar ratio: Mo:Fe:Mg=1:10:100	Temperature: 850 ^{o}C CH_4 flow: 45 sccm Ar flow: 150 sccm Purification: HCl, DI water	They observed time effect on the SWNT growth. When the synthesis time is less than 2 min, no SWNT growth occured. They obtained optimal results for 30 min growth time. After 40 min amorphous carbon was observed.

3.1.1.1. Literature Outcome

Majority of studies in the literature is about CNT growth. Several hydrocarbon gases were examined for CNT growth by CVD method. However, methane was reported to produce mostly SWNT material among them. Many catalysts are investigated for methane CVD and results show that mixture of transition metals are more efficient than monometallic catalyst for CNT growth. Especially, Fe-Mo and Co-Mo catalysts are reported for high quality CNT formation. Metal-supported catalysts are appropriate for CNT growth. As support, inorganic porous materials such as silica (SiO_2), alumina (Al_2O_3), zeolites and magnesium oxide (MgO) are generally used (Chai, et al. 2006).

Common catalyst preparation methods used for CNT growth are impregnation, sol-gel and combustion. Among these methods, impregnation method generally give SWNT and DWNT. The most promising support material is MgO for this method because of great number of alkaline reaction sites that it possesses. It gives high yield of SWNT and DWNT almost without any defect when it supported Fe-Mo bimetallic catalyst (Yoshihara, et al. 2007).

Sol-gel method produces catalysts with high surface area, high porosity and ultra-low density. The interaction between catalyst particles and support materials is very strong at this method, therefore it is also approriate for SWNT growth. Different from impregnation method, Al_2O_3 is the most efficient support for sol-gel method due to the strong Lewis acidity on the surface of Al_2O_3 material.

CNTs grown over catalyst produced by combustion method are generally MWNTs and they are thicker than CNTs grown over catalysts prepared by impregnation and sol-gel methods.

As a conclusion, Co-Mo/MgO catalyst prepared by gel-combustion method was chosen for this study, this method is a modified sol-gel method (Rashidi, et al. 2007). The advantage of this method is to give catalyst which has a high yield of surface area and give a good dispersion, that is why obtained CNTs are at high quality and high yield. In order to increase specific surface area, different organic compounds such as tartaric acid, citric acid, ethylenediamine tetraacetic acid (EDTA), and sorbitol can be used. Among these organic additives, sorbitol derived catalyst gives the highest specific

surface area and the smallest metal particle size (Rashidi, et al. 2007), therefore sorbitol was used in this study as a combustion additive.

3.1.2. The Nature of Metal

Their nanosized transition metal particles are generally used in CNT growth either in metallic or oxide forms. Transition metals possess some suitable properties for CNT production. These are melting temperature, equilibrium vapour pressure, solubility of carbon and carbon diffusion rate in the metal. But the most important property of the metals with regard to CNT formation is their ability to catalytically decompose gaseous carbon-containing molecules (Moisala, et al. 2003). In literature, different metal catalysts, e.g. La, Cu, Gd, MgO, Ni, Co, Fe, Pd, Cr, Mn, Zn, Cd, Ti and Zr have been used in order to find best catalyst for CNT growth, and among all Fe, Co and Ni transition metals and their compounds give best results. It was reported that carbon has a low solubility in Fe, Co, Ni metals at high temperatures and it leads to the metal-carbon solid state solutions formation (Dai 2002, Park, et al. 2002). The carbon solubility limit is between 0.5wt%-1.5wt% for a succesful catalyst (Vecchio and Deck 2006). It was also suggested that only d-electron transition metals are appropriate to use as a catalyst in CNT synthesis. With increasing number of unfilled d orbital number, the ability to bond with carbon atoms increases for transition metals (Arthur and Cho 1973). Fe, Ni and Co have few d-vacancies so they exhibit finite solubility for carbon at high temperatures.

Ago et al. examined the effect of Fe, Co, Ni catalysts on the synthesis of CNTs. The reasults revealed that the catalytic activity decreased with the species used in order of Fe > Co > Ni (Ago, et al. 2006). MgO was used as a support material, and Fe/MgO catalyst showed the highest methane conversion. The use of bimetallic catalyst increases the CNTs yield. Co-Mo (Alvarez, et al. 2001) and Fe-Mo (Harutyunyan, et al. 2002) are most common bimetallic catalyst for CNT growth. Mo also prevents sintering of the catalyst particles (Moisala, et al. 2003). Using a co-metal enhance the activity, stability and selectivity of the catalysts in CNT production. Comparing with single metals, bimetallic catalysts show a decrease in melting temperature and an increase in carbon solubility. Based on several studies, Co is the best catalyst in forming better quality CNTs (Hernadi, et al. 1996, Fonseca, et al. 1996, Ivanov, et al. 1994).

There are large number of studies in literature, about bimetallic (Fe/Co, Co/Ni, Fe/Ni, Fe/Mo, Co/Mo, Ni/Mo) and trimetallic (Fe/Co/Mo, Co/Ni/Mo, Fe/Ni/Mo) combinations of Fe, Co, Ni, Mo metals for CNT synthesis (Kathyayini, et al. 2008).

3.1.3. The Nature of Support Material

The most important function of support material is to provide high surface area and porosity for the active component. The interaction between catalyst and support material directly affects the dispersion and morphology of catalyst. Active component must be dispersed over support material in such a way that sintering is reduced. Either chemical or physical interactions can occur between support and metal. Van der waals and electrostatic forces are the physical forces that prevent catalyst particle movement on the support surface. These forces also reduce thermally driven diffusion and metal particle sintering on the support material. Hence, catalyst particle size distribution is achieved during CNT sythesis (Moisala, et al. 2003). Chemical interactions also take place in the stabilization of size distribution. But when chemical interaction is very strong, particle mobility decreases, and it limits the particle coalescence.

In CNT growth, the catalyst needs an appropriate support material for selectively controlling the morphology and the yield of CNTs. Alumina (Su, et al. 2000), magnesium oxide (Yoshihara, et al. 2007), silica, titania, and zeolites are commonly used as a support. Chai et al. investigated effects of different support material on CoO catalyst (Chai, et al. 2006). They examined silica, titania, ceria, magnesia, alumina, zeolite, and calcium oxide supports, using methane as a carbon precursor. They found that at 700 ^{o}C growth temperature, the carbon capacity decreased in order of alumina > ceria > zeolite > silica > titania > calcium oxide > magnesia. In an other study, Qingwen et al. examined silica, alumina, magnesium oxide, calcium oxide and zirconium oxide under the same experimental conditions and using Fe and Mo (Quingwen, et al. 2002). Their Raman characterization results showed that there was no SWCNT formation on silica, zirconium oxide and calcium oxide supported catalysts. Alumina and magnesium oxide gave SWCNTs but among these support materials magnesium oxide was the most efficient in the production of SWCNTs. MgO possesses a great number of alkaline reaction sites, and some metal oxides have been verified to be able to disperse well over it even at high temperatures (Wang, et al. 1998). An other

advantage of MgO support is that it can be be removed easily with a mild acid treatment.

3.2. Catalyst Preparation Methods

Catalyst preparation method is also very important in CNT growth. There are numerous catalyst preparation methods. This section covers four main catalyst preparation methods for CNT growth including impregnation, precipitation, combustion, and sol-gel methods.

3.2.1. Impregnation Method

Impregnation is the simplest and most direct method of deposition. In this method, in order to give the correct loading, the pores are filled with a sufficient concentration metal salt solution (Richardson 1989). In other words, a catalyst precursor dissolves, and then the whole precursor deposits into the support. At the next step, solvent is evaporated and dried (Venegoni, et al. 2002). During drying, crystallization of the salt occurs on the pore surface, therefore, if this step does not perform properly, an irregular concentration distribution might occur. Crystallization should be slow enough to form uniform deposits (Richardson 1989). The last step in catalyst preparation by impregnation method is the calcination. Crystallized salt redisolves when the dehydrated catalyst is exposed to moist environment and subsequent process drying may violate optimum conditions. Calcination converts the salt to an oxide or metal and essentially stops the distribution. Drying and calcination steps are very important because of the tendency towards egg-shell catalyst and risk of sintering interaction compounds and bursting of support.

The impregnation method is very fast compared with other catalyst preparation methods. The final properties and configurations of the catalyst can be controlled in this method. However, there is an disadvantage of impregnation method; it is very hard to obtain a high concentration catalyst. There are three different methods available to deposit the catalyst on the surface skin of the pore structure (egg shell) or into the inner pore structure (egg yolk) by a competitive chemisorption of special adsorbate. For this, formic acid, citric acid or hydrochloric acid can be used.

In the case of a organic support and molecules, one speaks about incubation (Li, et al. 2001), but the method remains the same.

3.2.2. Precipitation Method

The aim of precipitation method is to achieve a reaction of the type;

Metal salt solution + Support $\xrightarrow{\text{Base}}$ Metal hydroxide or Carbonate on support (Richardson 1989)

In this method, firstly, a metal salt, X_mY_n, solution is prepared, which will turn into the metal oxide M_xO_y. Powders or particles are slurred with an amount of this salt solution sufficient to give the required loading. Applying preliminary heating or evacuation makes easier to properly fill the pores with the solution. Most common solvent used to prepare this solution is water, but if necessary organic solvents can be used. The quantity of oxide desired determines the amount of solvent.

In order to precipitate the solution, enough alkali solution should be added. After precipitation, the powder is separated and washed in order to remove alkali ions, reagent anions, and excess deposit on the outside of the particles. Deposition occurs at two steps; firstly sols precipitate in bulk and pore fluid, and then interact with support surface. If OH groups of the support surface enter into reaction so that the pH of the surface region is higher than in the bulk solution, best results can be obtained. Then, precipitation occurs preferentially and uniformly on the surface.

Rapid nucleation and growth in the bulk solution may cause sols to be too large to enter the pores readily and associate only with the outside of the particle, so it should be prevented. This is most likely to occur in the vicinity of the alkali droplets entering the solution. Rapid mixing is very important. Dilute alkali may be added, drop by drop, with rapid agitation to disperse the droplets before local concentrations become excessive. Alternatively, both the salt and alkali mixed in a container of water (Stiles 1983).

To control uniform precipitation, urea can be used rather than conventional alkalis. Urea dissolves in water but decomposes very slowly above 90^{o}C. Urea is added to the metal salt-support solution and the solution heated while stirring. At 90^{o}C, urea hydrolyzes and OH groups are formed uniformly throughout the pores. Precipitation takes place homogenously over the surface. Since hydrolysis is slow and precipitation is

rapid, OH groups are consumed as soon as they are formed and the pH of the solution remains unchanged. This technique gives very uniform product, and can be easily scaled-up (Hermans, et al. 1979).

At the next step the solution is added to distilled water for washing and mixing. As standing particles settling slowly desorbe foreign ions as they fall. (When a definite interface is visible, water is removed by decantation and the pores repeated.) After washing, the precipitate is filtered.

At the final step, the treated support is dried to remove excess moisture from the pores. This operation is not critical as support preparation step, since the active component is firmly anchored to the surface. However, precautions should be taken to avoid rapid heating which generates large internal steam pressures. Beyond heat treatment, drying procedure is called as calcination. Calcination process decomposes the deposited hydroxides and cabonates into stable oxides or metals, depending on the atmosphere. At this process pore size distribution changes, active phase generation and surface reconditioning occurs, and mechanical properties stabilizes.

Precipitation is the preferred deposition route for loadings higher than 10%-20%. Below this value, other techniques are usully practiced (Richardson 1989).

3.2.3. Combustion Method

In combustion method, a solvent and metal salts which are the precursors of the catalyst are mixed. Water is used as common solvent for this method; however, ethanol or another organic materials can also be used as solvent material. The mixing process is made at room temperature to provide uniformly dispersion for metal salts. There are different organic additives used for combustion such as citric acid, polyethylene glycol (PEG), sorbitol, tartaric acid and ethylenediamine tetraacetic acid (EDTA) (Rashidi, et al. 2007). After enough mixing the sample becomes gel-like. In this method, the last step is the combustion of gel-like sample at high temperatures. The combustion is generally made under 500-600 ^{o}C for 5-15 min. in a pre-heated oven (Flahaut, et al. 2004).

3.2.4. Sol-Gel Method

Sol-gel is a process in which a gel is formed from the particles of a sol when attractive forces cause them to stick together in such a way as to form a network (Regalbuto 2007). In other words, sol-gel process is the formation of a gel by aggregation of particles in a sol. This process has some remarkable properties such as high dispersion of metal or alloy, high porosity, easy mass transfer and thermal stability, and its preparation is easy, so sol-gel supported metals are appropriate as catalysts. Stronger anchoring of metal particles in the pores of the support is also often observed (Ward, et al. 1995, Heinrichs, et al. 1997, Ji, et al. 2001) and this may provides a higher stability at a high temperature.

3.2.4.1. Dissolution of Metal Salts in the Precursory Sol-Gel Solution

The synthesis of a support by the sol-gel method starts with preparation of homogeneous solution of precursors of that support, so an adequate precursor of the active species can be dissolved in that solution (Mehn, et al. 2004, Su, et al. 2000)

The aim is to try to include the active metal precursor in the porous growing gel without making it inaccessible in the final catalyst. The metal to be highly dispersed is to maintain the metal precursor in solution at the sol-gel step, this is sometimes difficult with noble metals, since they are easily reduced and then precipitated.

If metals are supported on inorganic gels, a salt of the desired metal, which is soluble in the initial sol-gel solution whose solvent most often is an alcohol, can be found (Kukovecz, et al. 2000). It is also possible to realize a dissolution of the metal salt in an adequate solvent and to add that metal precursor solution to the sol-gel solution (Armor, et al. 1985). The preliminary dissolution of the metal salt in the water which will be used to hydrolyze the support precursor alkoxyde is often encountered (Lopez, et al. 1991).

Metal precursors in the dissolution method do not participate directly in the sol-gel chemistry involving the oxide precursors which are usually alkoxides. In the dissolution method, the metal precursor is often simply encapsulated in a growing gel network, but its presence can still indirectly influence the sol-gel process (Ward, et al. 1995) and leads to modifications in the structure of the final catalyst.

3.2.4.2. Cogelation of Metal Chelates with Support Precursors

Cogelation method consists of using an alkoxysilane-functionalized ligand of the type (RO)3Si-X-L in which the ligand L, able to form a complex -LNM with a metal M (M = Pd, Ni, Ag, Cu, etc.), is connected to the alkoxide moiety (RO)3Si- via an inert and hydrolytically stable tethering organic group X. The concomitant hydrolysis and condensation of such molecules with a network-forming reagent such as Si(OC2H5)4 (TEOS), i.e. their cogelation, result in materials in which the catalytic metal is anchored to the SiO_2 matrix (Deschler, et al. 1986, Breitscheidel, et al. 1991).

In general, the alkoxysilane-functionalized metal complex is formed from a metal precursor and an alkoxysilane-functionalized ligand in a solvent (most often in ethanol) before adding the silica precursor and water for gel formation. Examples of metal precursors are acetates ($Pd(OAc)_2$, $Co(OAc)_2$, $Cu(OAc)_2$, $Ni(OAc)_2$, Ag(OAc), etc.) acetylacetonates ($Pd(acac)_2$, $Pt(acac)_2$, etc.), and nitrates ($AgNO_3$, etc.).

Contrary to the metal precursor in the dissolution method, once formed, the alkoxysilane-functionalized metal complex is directly involved in the sol-gel chemistry. Indeed, as the main SiO_2-network forming reagent ($Si(OR)_4$), this complex undergoes hydrolysis and condensation. Besides its anchoring function, the alkoxysilane-functionalized ligand presents two particularly interesting advantages for preparing metal containing as well as pure silica gels firstly it allows the solubilization of metal salts that are insoluble in alcohol, and whereas attempts to synthesize a pure silica gel by the same method as cogelled Pd/SiO_2 samples failed (Heinrichs, et al. 1997), the introduction of ligands such as [3-(2-aminoethyl)aminopropyl] trimethoxysilane makes such a synthesis possible (Lambert, et al. 2004). Therefore, the use of such ligands allows to prepare pure silica gels by a way other than the usual acid-base method (Brinker, et al. 1982).

Physico-chemical characterization of cogelled catalysts indicates that the introduction of alkoxysilane-functionalized ligand in the sol-gel solution influences strongly the characteristics of the final material. These catalysts exhibit a very particular structure leading to remarkable properties.

3.2.4.3. Drying of Wet Gel

High porosity is an important parameter for an efficient heterogeneous catalyst, so it should be maintained as high as possible in the dried gel. Depending on whether the liquid in the wet gel is removed by evaporative drying or by supercritical drying, that is in pressure and temperature conditions beyond the critical point of the liquid, the resulting dry material is named xerogel or aerogel respectively. A third class of materials are cryogels dried by freeze-drying or lyophilization (Pajonk 1997).

Supercritical drying has been generally used to remove alcoholic solvent in inorganic wet gels. In order to obtain critical conditions, autoclave is used. The critical conditions are T_c = 514 K and P_c = 6.1 MPa for ethanol. The high-pressure system is flushed with nitrogen, fully closed, and heated slightly above the critical point of the solvent used. Then, the pressure is released and the autoclave is flushed with nitrogen to remove residual alcohol and lastly cooled to ambient temperature (Schneider, et al. 1995). Obtained porous materials after this process are called as aerogels (Pirard, et al. 1997). While maintaining very large pores, supercritical drying in alcohol can cause the closing of micropores and thus make an aerogel catalyst completely inactive because of active metal particle occlusion (Heinrichs, et al. 1997).

Scaling-up at an industrial level is not possible for such a high-temperature process, therefore a low temperature supercritical drying in carbon dioxide has been developed. In this procedure, the advantage is the low critical temperature of CO_2. Using this drying process involves a solvent exchange by liquid CO_2 before achieving the drying step (Pajonk 1997, Schaefer, et al. 1995). Supercritical drying conditons are T_c = 304 K, P_c = 7.4 MPa for CO_2. When drying is achieved with this process, a solvent exchange by liquid CO_2 takes place before achieving the drying step (Suh, et al. 1998).

Freeze drying is another possiblity for drying. At this process the pore liquid is frozen into a solid, then sublimes and gives an aerogel-like material which is called a cryogel (Ko, et al. 1997). Freze drying is used for organic gels synthesized in a aqueous medium (Mathieu, et al. 1997) and inorganic gels which are prepared in alcoholic medium (Mehn, et al. 2004).

CHAPTER 4

EXPERIMENTAL

Experimental study details are given in this chapter. In the first section, nanocatalyst particles preparation by gel-combustion method was explained, and in the second part CNT growth by thermal chemical vapor deposition (TCVD) method is explained. The last section is focusing on characterization techniques which are SEM, TGA, TEM, XRD and Raman Spectroscopy.

4.1. Catalyst Preparation Process

In this work, catalyst particles synthesized by gel-combusition method was used. This method has some advantages; it gives high specific surface area and good dispersion of the active sites for catalyst, and hence obtained CNTs have high yield and high quality.

Co-Mo/MgO catalyst was prepared using gel-combustion method with sorbitol as organic additive and analyzed in order to find the most efficient pretreatment and growth conditions for high quality CNT growth. To produce Co−Mo/MgO catalyst, $Co(NO_3)_2.6H_2O$, $(NH_4)_5Mo_7O_{24}.4H_2O$, and $Mg(NO_3)_2.6H_2O$ salts with a molar ratio of Co:Mo:MgO;0.5:0.25:10 and sorbitol were dissolved in 10 ml distilled water by stirring until a clear solution was obtained. The solution shown in Figure 4.1(a) was dried at 100 ^oC for 3 hours to form a uniform gel (Figure 4.1(b)), followed by a flash calcination of obtained gel in oven at 550 ^oC for 30 minutes. Then it was ground into a powder with particle sizes between 75-250 μm. Final form of Co-Mo/MgO catalyst was shown in Figure 4.1(c).

(a) (b)

(c)

Figure 4.1. a) initial solution, b) obtained gel after drying, c) Co-Mo/MgO catalyst for CNT growth

4.2. CNT Growth Process with Thermal Chemical Vapor Deposition Method

In this study TCVD method was used to sythesize CNT. The TCVD system used for this study can be seen in Figure 4.2. The system consists of two parts, first part is a Lindberg/Blue M 1100 ^{o}C Split Mini Furnace and the other part is its controller. All expriments were done at a high temperature so samples in a quartz boat were placed in a 1 inch diameter quartz tube. The upper temperature limit of the furnace is 1100 ^{o}C .

Figure 4.2. The TCVD system, CNL Lab in Physics Department IYTE

Figure 4.3. Quartz boat used to carry catalyst particles into oven

In this study, CNT growth experiments were performed at atmospheric pressure. Firstly, a catalyst pretreatment took place with Ar, H_2 or Ar-H_2 mixture keeping the total gas flow at 200 sccm for 1 hour at 850 ^oC. Ar gas sent into the system to remove the contamination and to prevent the oxidation of the samples, and H_2 gas sent into the system to prevent amorphous carbon formation and to provide the reduction from metal oxide catalyst to metal catalyst which are more suitable for CNT growth. After reaching to the desired temperature CH_4 gas flow was started to initiate CNT growth. Ar and H_2 continued to flow during CNT growth. The total gas flow was 250 sccm at growth. Different gas flow rates for Ar, H_2 and CH_4 were investigated. In this study growth temperature in the range of 850 to 1000 ^oC was studied.

Growth time was also another parameter for the CNT growth, 5 different growth times were investigated, 5 min, 10 min, 20 min, 30 min and 40 min.

When the growth was finished, first the hydrocarbon gas was turned off but H_2 gas and Ar gas was stil flowing through the system and the temperature was setted to 0 ^{O}C so the system was left for cooling under again Ar, H_2 or Ar-H_2 mixture ambient. Some of as-grown CNTs were purified with 4M HCl acid treatment. The growth conditions studied are listed in the Table 4.1.

Table 4.1. Growth conditions of CNTs in TCVD method

Sample Name	Catalyst Pretreatment Conditions		CNT Growth Conditions				
	H_2 (sccm)	Ar (sccm)	CH_4 (sccm)	H_2 (sccm)	Ar (sccm)	Time (min)	Temperature (^{o}C)
CNT513	200	-	50	200	-	40	1000
CNT518	150	-	50	150	-	40	1000
CNT523	100	-	50	100	-	40	1000
CNT524	200	-	50	200	-	40	850
CNT525	200	-	50	200	-	40	900
CNT526	200	-	50	200	-	40	950
CNT527	-	200	50	200	-	40	1000
CNT528	50	150	50	200	-	40	1000
CNT 529	200 at 850 ^{o}C	200 (until 850 ^{o}C)	50	200	-	40	1000
CNT530	200	-	50	50	150	40	1000
CNT531	200	-	20	20	210	40	1000
CNT532	-	200	20	20	210	40	1000
CNT533	10	190	20	20	210	40	1000
CNT534	200 at 850 ^{o}C	200 (until 850 ^{o}C)	20	20	210	40	1000

(cont. on next page)

Table 4.1 (cont.)

CNT535	200	-	40	-	210	40	1000
CNT536	-	200	40	-	210	40	1000
CNT585	10	190	40	-	210	40	1000
CNT601	200 at 850 ^{o}C	200 (until 850 ^{o}C)	40	-	210	40	1000
CNT 606	200	-	50	200	-	30	1000
CNT609	200	-	50	200	-	20	1000
CNT 615	200	-	50	200	-	10	1000

4.3. Characterization Techniques

This study is a parametric study whose aim is to find optimal growth and pretreatment conditions for high quality and high yield, therefore, through characterization of obtained CNTs is essential. In this study, the catalyst was characterized by X-ray diffraction (XRD), N_2 adsorption (BET surface area) and scanning electron microscopy (SEM), and purified and unpurified CNT samples were analyzed with SEM, thermo-gravimetric analysis (TGA), Raman spectroscopy, and transmission electron microscopy (TEM).

4.3.1. Scanning Electron Microscopy

SEM (Scanning Electron Microscopy) images the sample morphology by scanning the surface with a high energy beam of electrons. SEM is the first step to characterize the CNTs. Using SEM, morphology of CNTs, their dimensions and their orientations can readily be seen (Thess, et al. 1996, Liu, et al. 2004, Li, et al. 2002). Diameters of CNTs also can be measured roughly with SEM.

Sending an electron to the specimen surface, several signals can be detected. When the primary electron is sent, high energy backscattered electrons appear and

primary electron can be diffracted with large angles. secondary electrons are generated when these backscattered electrons emerge from the surface. These secondary electrons have energies between 0 and 20 eV, and can be attracted to a positively charged detector with high efficiency. Comparing primary elctrons number, the secondary electron number is high and increases as the angle φ between the electron beam and the surface normal increases in proportion to 1/cosφ [surface analysis methods in material science].

There is a large annular detector below the final lens, facing towards the sample and a proportion of the scattered electron signal can be collected with this detector. With increasing atomic number Z of an elemental sample, the scattering of primary electrons increases. Depending on the surface composition and orientation between the electron beam and surface, the backscattered electron signal from a flat, polished sample provides contrast.

The resolution of the backscattered electron image is typically in the range between 0.1-1 μm, but it is possible to image very finely spaced regions showing compositional contrast at resolutions down to 2-3 nm using high brightness guns and efficient backscattered electron detectors. There is a small high resolution component in the backscattered signal and it is generated by incident beam electrons being scattered out of the sample very early in their path. The resolution of the whole backscattered signal can be improved by reducing the beam energy but the detectors become less efficient for the lower energy electrons, and so this is not appropriate.

The SEM utilized for this study was a Philips XL 30S-FEG.

4.3.2. Transmission Electron Spectroscopy

The internal microstructure and crystal structure of samples which are thin enough to transmit electrons can be analysized with Transmission Electron Microscopy (TEM). TEM is used to measure outer and inner radius and linear absorption coefficient for CNT studies. It is the most useful instrument in order to determine the diameter of SWNTs and MWNTs and the number of walls. The intershell spacing of MWNTs (Kiang, et al. 1998) also is studied with high resolution TEM and found between the range of 0.34-0.39nm. An other subject studied with TEM is SWNT's helicity (Cowley, et al. 1997, Qin, et al. 1997, He, et al. 1998).

There are a series of magnetic lenses in TEM after electron gun to provide a uniform illumination of the specimen over the area of interest. The sample is mounted on a stage to provide suitable movement. The primary image is formed by the objective lens. This objective lens determines the final resolution. The final image is projected onto a viewing screen through two or more projection lenses, and can be recorded.

4.3.3. Raman Spectroscopy

Micro-Raman spectroscopy is generally used to study the quality of CNTs. This technique gives information with details about configuration of CNTs. Number of walls, the presence of crystalline and amorphous carbon and diameter of SWNTs can be determined with the Raman spectroscopy.

When a beam of light passes through a transparent sample of a chemical compound, a small part of the light emerges in different directions than the incoming beam. Most of these scattered light is of unchanged wavelength, however a small part has wavelengths different from the incident light, and its presence is a result of Raman effect. The pattern of the Raman spectrum is characteristic for every molecular species and the intensity is proportional to the number of scattering molecules in the path of the light. Resonance peaks are also observed in the spectrum, which symbolyze the presence of a particular specie type that is in abundance.

The characteristic spectrum of SWNTs includes three main zone. At low (100-250 cm^{-1}), intermediate(300-1300 cm^{-1}) and high(1500-1600cm^{-1}) frequencies (Journet, et al. 1997, Colomer, et al 2000).

There are two main first order peaks for carbon-based materials. The first one is the D peak, it is observed around 1300 cm^{-1} for excitation He-Ne laser, or at 1350 cm^{-1} for an Ar ion laser. The D peak shows the presence of defects (Geng, et al. 2002). The other one is the G peak and observed at about 1580 cm^{-1}, which is related to the in-plane vibrations of the graphene sheet (Singh, et al. 2003, Shanov, et al. 2006). Ratios of the D peak to the G peak is significant for CNT characterization because it gives the amount of disorder within nanotubes (Tans, et al. 1997). A small I_D/I_G ratio, in the range of 0.1-0.2, indicates that the defect level in the atomic carbon structure is low, and it means that reasonable crystalline quality observed (Singh, et al. 2003).

Low energy peaks around 191 and 216 cm^{-1} are the radial breathing modes of CNTs (Rao, et al. 1997), and can be clearly observed using He-Ne laser (Lee, et al. 1997). The spectrum in the low frequency domain reflects the SWCNT diameter and can be used to calculate it. In general, the frequency increases with decreasing tube diameter (*d*). The frequency *v* of these modes is inveresly proportional to the diameter of the SWCNT. The diameter of the SWCNT can be determined using equation below (Shanov, et al. 2006),

$$v\ (cm^{-1}) = 223.75 / d\ (nm) \quad \text{(Eq. 4.1)}$$

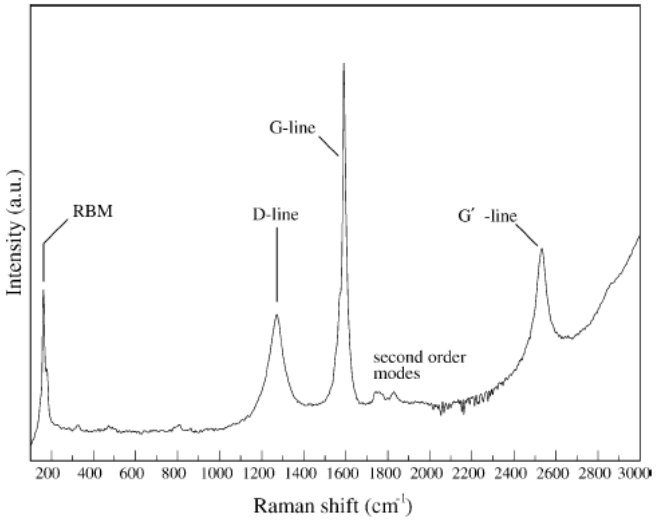

Figure 4.4. Raman spectrum showing most characteristic features of CNTs (Source: Belin and Epron 2005)

4.3.4. Thermogravimetric Analysis

Thermogravimetric analysis (TGA) method is performed on samples to determine weight loss or gain by changing temperature. Every element shows different behaviours, for this reason their weight losses are different depending on temperature, so TGA is used to determine characteristics of materials. Matching with standarts is necessary for identification. Additional information can be obtained by using different reactive atmospheres, such as hydrogen, oxygen and H_2S. The technique with hydrogen, cold temperature programmed reduction (TPR) gives information about the reducibility of oxides. Catalysts that are easier to reduce for examples in which oxides are bound less strongly to the support show reduction peaks at lower temperatures.

CNT has a different oxidation temperature that the other carbonaceous product. The oxidation temperature of amorphous carbon is between 200 ^{o}C and 450 ^{o}C (Kong, et al. 1998), and SWCNTs and MWCNTs are oxidized between 500 ^{o}C and 800 ^{o}C in air (Dai, et al. 1996). But these temperature ranges can change with atmosphere, heating and the presence of metallic particles between the catalyst.

In this study, a Perkin Elmer-Diamond TGA was used. For these analysis CNTs were put into a platinum crucible, and heated from 25 ^{o}C to 800 ^{o}C with 10 ^{o}C/min ramp rate, under nitrogen flow.

4.3.5. X-Ray Diffraction for Catalyst Characterization

In X-ray diffraction system, electrons emitted from the filament (cathode) are accelerated to target (anode) and X-rays characteristic of atoms in the irradiated area are emitted. By analyzing their energy, the atoms can be identified and by counting emitted X-rays number, the atom concentration in the specimen can be determined.

X-ray diffraction (XRD) is mostly used for bulk structure analysis. Hovewer, if the concentration of active component is large enough, it can be appropriate for size determination. Quantitatively, a number average size is obtained from the equation below (Richardson, et al. 1989)

$$d = \frac{0.85\lambda}{(B^2 - b^2)^{1/2}\cos\theta} \qquad \text{(Eq. 4.2)}$$

where B is the peak width for a diffraction line at angle θ, b is the value for a well crystallized specimen, and λ is the wavelength.

CHAPTER 5

RESULTS AND DISCUSSION

First section in this chapter focuses on Co-Mo/MgO catalyst characterization. SEM was used to determine catalyst morphology and X-ray diffraction method was used to determine the catalyst crystallinity. In the second section CNT growth results are analysed to determine optimal parameters for CNT growth. Different parameters were studied in this work to find the optimal conditions. In this section firstly, CNT growth and pretreatment atmosphere is discussed to obtain high quality CNT. After determining best pretreatment and growth atmosphere; in the following section the effect of hydrogen flow rates on the CNT growth is examined, and this followed by a part which is about the effect of growth temperature on the yield and quality of CNTs. At the last part, growth time effect on CNTs is discussed. For this discussion, SEM, TEM, TGA, and Raman spectroscopy characterization techniques were used.

5.1. Characterization of Co-Mo/MgO Catalsyt

Catalyst material is one of the most important parameter in CNT growth process, since the catalyst affects the size of CNTs, the diameter of a CNT is directly proportional to nanocatalyst particle size and determines also the wall number, hence, the type of CNT. As explained beforehand, only transition metals are suitable for effective CNT growth as a catalytic material, and Fe, Co, Ni are the most common and effective catalysts. In this thesis work, Co-Mo/MgO catalyst was used. The produced catalyst must have some properties which are significant for CNT growth. A catalyst should have a high surface area and it should show high active sites dispersion. The following SEM images and XRD scan give information about the catalyst obtained and used for CNT growth in this study.

Figure 5.1 and Figure 5.2 show SEM images at different scales and XRD scan of the Co-Mo/MgO catalyst. From SEM images it was observed that catalyst material consist of quite large particles. Particles sizes were in the range of 75- 250 μm. XRD scan gave wide peaks, which means that catalyst had small crystallite sizes. There was

no observable peak for Co or Mo, only one phase could be identified; all XRD peaks belong to MgO. This indicates that Co and Mo loading is on a small scale and these metals show high dispersion. The high dispersion is generally consistent with high surface area.

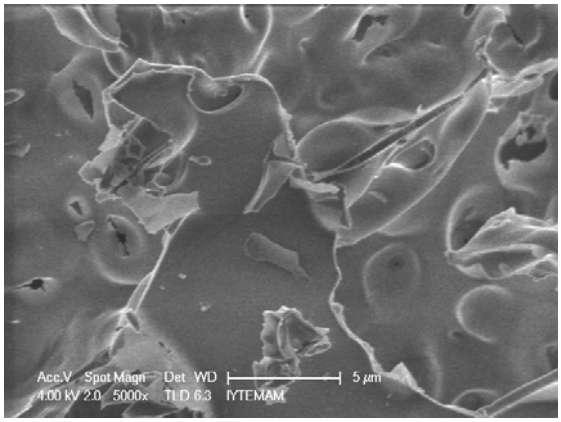

(a)

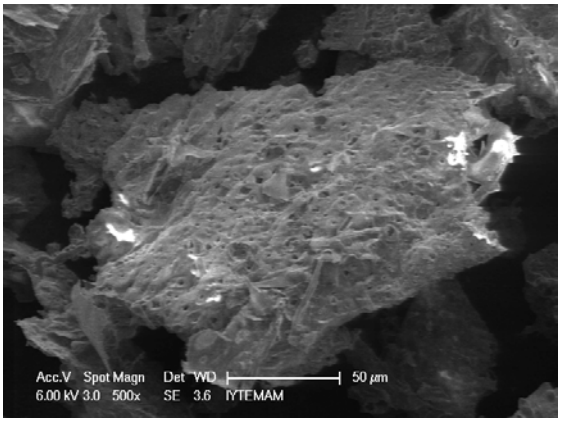

(b)

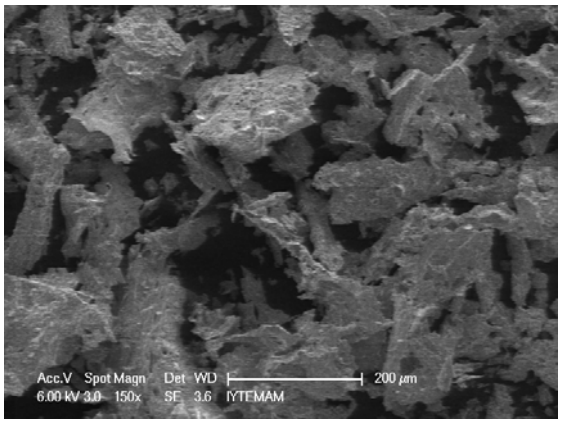

(b)

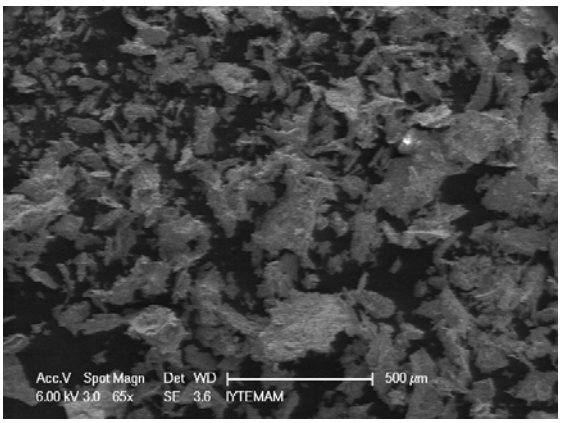

(d)

Figure 5.1. SEM micrographs of Co-Mo/MgO catalyst at a) 5 μm scale 319 b) 50 μm scale c) 200 μm scale d) 500 μm scale

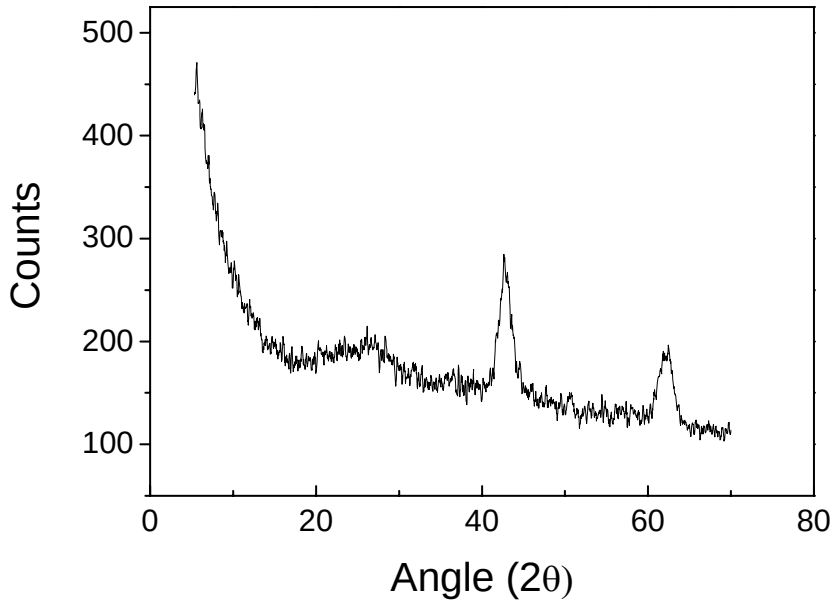

Figure 5.2. XRD scan of Co-Mo/MgO catalyst

BET surface area of Co-Mo/MgO catalyst prepared with combusition method using sorbitol as an organic additive was given in literature as 205 m^2g^{-1} (Rashidi, et al. 2007).

5.2. Characterization of Carbon Nanotubes

5.2.1. CNT Formation at Different Pretreatment and Growth Atmosphere Composition

Well controled ambient is important for obtaining high quality end product. Commonly used ambient gases are nitrogen, hydrogen and argon for CNT growth in the literature. Ambient gas effect is to control the decomposition rate in the growth process.

Three different growth conditions were investigated in this section. Methane was used as a carbon source for all experiments, however diluting gas(es) was varied. Argon, hydrogen and a mixture of the two gases were added to methane to adjust partial pressure of carbon source and control the deposition rate. For all of the three growth conditions, four different pretreatment processes were investigated. Pretreatment lasted for one hour at 850 ^oC. First, effect of hydrogen on CNT characteristics was examined, H_2 flow rate fixed at 200 sccm flow rate, then effect of argon was examined with again 200 sccm flow rate. The third pretreatment included both argon and hydrogen gases at

the same time. For these three pretreatment conditions heating and cooling process also took place with the same gas rates continued to flow during pretreatment. However, the last pretreatment conditions was slightly different from the others. There, pretreatment was done with hydrogen gas at 850 ^{o}C for just one hour, and for heating and cooling processes argon flow took place.

5.2.1.1. CNT Growth Under H_2 Ambient

In the first growth conditions, hydrogen was flowed with methane. Growth conditions were CH_4=50 sccm, H_2=200 sccm and T=1000 ^{o}C and four pretreatment conditions were examined.

Table 5.1. Studied pretreatment conditions for the first growth scheme.

CNT number	Hydrogen (sccm)	Argon (sccm)
CNT 513	200	-
CNT 527	-	200
CNT 528	50	150
CNT 529	200 (for 1h at 850 ^{o}C)	200 (until 850 ^{o}C)

SEM pictures of the as grown samples in hydrogen atmosphere for different pretreatment conditions are given in Figure 5.3. For the growth in hydrogen atmosphere, when we used 200 sccm H_2 in pretreatment process, CNTs with high purity and average diameter of 8.3 nm were obtained (Figure5.3a). When 200 sccm argon, instead of H_2, sent to the system for pretreatment average diameter increased to 13.1 nm and different carbon structures were observed due to some impurities. In the pretreatment conditions when argon and hydrogen was sent to the system as a mixture and as-grown CNTs average diameter was 9.9 nm (Figure 5.3(c)) but CNTs were tangled compared to those obtained from hydrogen alone pretreatment conditions. The last pretreatment results gave the thickest CNTs with 19.5 nm but they were not tangled.

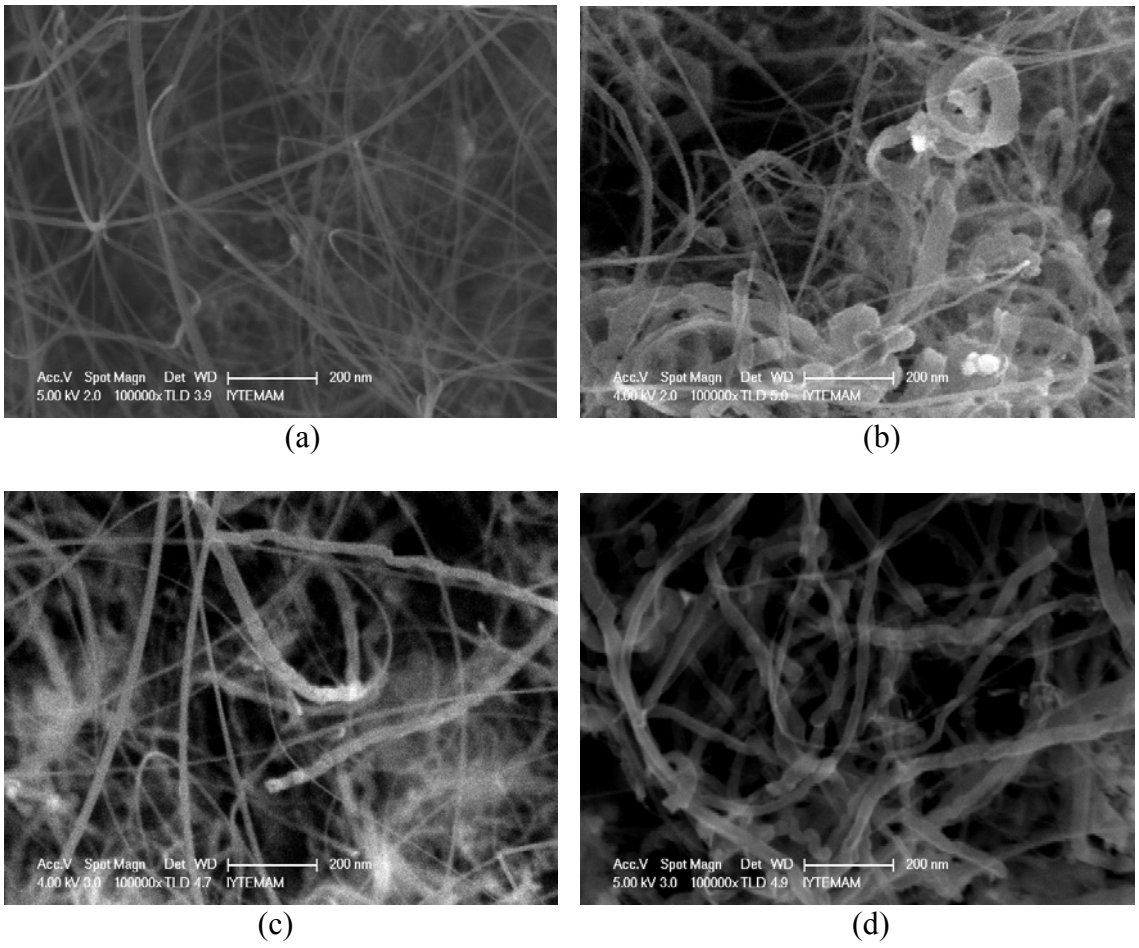

Figure 5.3. SEM micrographs of (a) CNT 513 (b) CNT 527 (c) CNT 528 (d) CNT 529

Due to CNT's unique properties, they are used in many applications and some of these applications require large scale growth of CNTs. So, in this study, the other aim was to produce large amount of product for given amount of catalyst. The total yield of CNTs can be calculated using (Rashidi, et al. 2007);

$$Yield = \frac{(W_{product} - W_{catalyst})}{W_{catalyst}} \times 100\% \qquad \text{(Eq.5.1)}$$

In order to calculate CNTs average diameter, large number of CNT diameters were measured and then the arithmetic average was calculated.

Table 5.2. Yield and size of CNTs for the first growth conditions

Sample Name	Pretreatment	Mass Before CNT Growth (mg)	Mass After CNT Growth (mg)	Yield %	Average Diameter (nm)
CNT 513	H_2 Only	50.2	197.0	292.4	8.3
CNT 527	Ar only	15.5	30.0	93.5	13.1
CNT 528	Ar+H_2	15.0	51.5	243.3	9.9
CNT 529	H_2 for only one hour	15.2	25.4	67.1	19.5

The highest yield using Eq.5.1 was obtained in pure hydrogen atmosphere with 292.4% (Table 5.2). In addition, argon-hydrogen mixture pretreatment also gave high yield compared to the other two conditions. The yields were below 100% for the second (CNT 527) and fourth (CNT 529) pretreatment conditions. In terms of CNT yield and structural quality, for this growth condition, pretreatment in pure hydrogen atmosphere had the highest yield, smallest average diameter and least amount of purities (as observed from SEM).

Thermogravimetric analysis was done to analyse thermal properties of CNTs. TGA curves of as grown samples were taken without any purification. CNT has a different oxidation temperature that the other carbonaceous product. The oxidation temperature of amorphous carbon is between 200 ^{o}C and 450 ^{o}C, and SWCNTs and MWCNTs are oxidized between 500 ^{o}C and 800 ^{o}C in air. TGA results indicated that there was almost no amorphous carbon formation under first, second and fourth pretreatment conditions, but under argon-hydrogen pretreatment atmosphere a weight loss step was observed in the temperature range 200-500 ^{o}C which means some amorphous carbon coating on CNTs were generated when they are grown. As-grown CNTs under argon, hydrogen mixture pretreatment shows 87.7 % purity value, there is 12.3 % amorphous carbon. TGA curves of hydrogen rich growth condition were given in Figure 5.4.

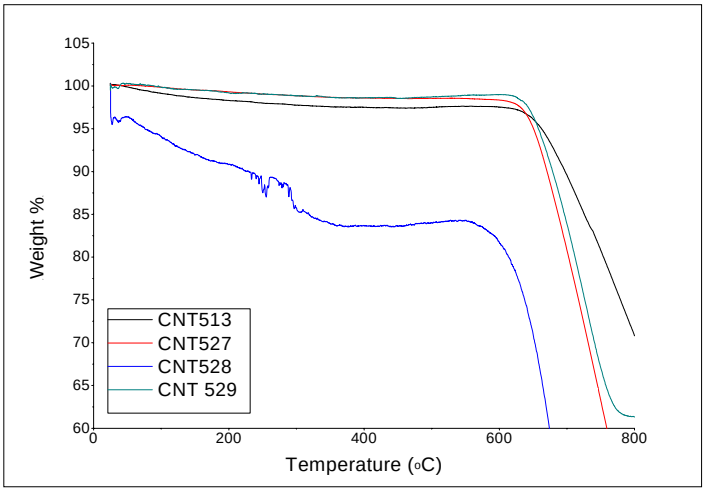

Figure 5.4. TGA diagrams of as grown samples in hydrogen rich growth condition

As shown in Table 5.3 the lowest amorphous carbon weight was observed under H_2 only pretreatment atmosphere and the highest transition temperature also was observed for this sample. Transition temperature depends on the graphitization level of CNTs. Amorphous carbon burns at lower temperature than CNTs because of its weaker bounds. Raman results supported TGA results and the lowest I_D/I_G ratio was calculated for H_2 only pretreatment which indicated that the lowest disorder occurred for this condition.

Table 5.3. Amorphous carbon amount and Raman I_D/I_G Ratio of CNTs for the first growth conditions

Pretreatment	Amorphous carbon %	Transition Temp.(^{o}C)	Raman I_D/I_G Ratio
H_2 only	0.6	649	0.16
Ar only	2.5	631	0.23
H_2-Ar	12.3	597	0.21
Ar than H_2	1.2	640	0.32

Transmission electron microscopy was used to analyse the structural quality of CNTs namely inner and outer diameters, number of walls and defects. In this study, TEM characterization of samples were carried out in UNAM, in Bilkent University. For TEM analysis, sample preparation is a significant step. CNTs were suspended in ethanol to carry then to a TEM grid. Samples were put in a 99.9% purity ethanol and then they were sonicated for 1 hour for uniform distribution. However, amorphous carbon film coatings were seen over and in between CNTs after ethanol evaporation. This film time to time prevented observation of the nanotubes clearly.

TEM images of CNTs grown under hydrogen rich atmosphere indicated that Co-Mo/MgO catalyst yielded a high nanotube density (Figure 5.5b). There were CNTs with different wall number, inner and outer diameter. CNTs shown in Figure 5.5 were all multi wall, however, this was not a general result because we could get only limited number of TEM images.

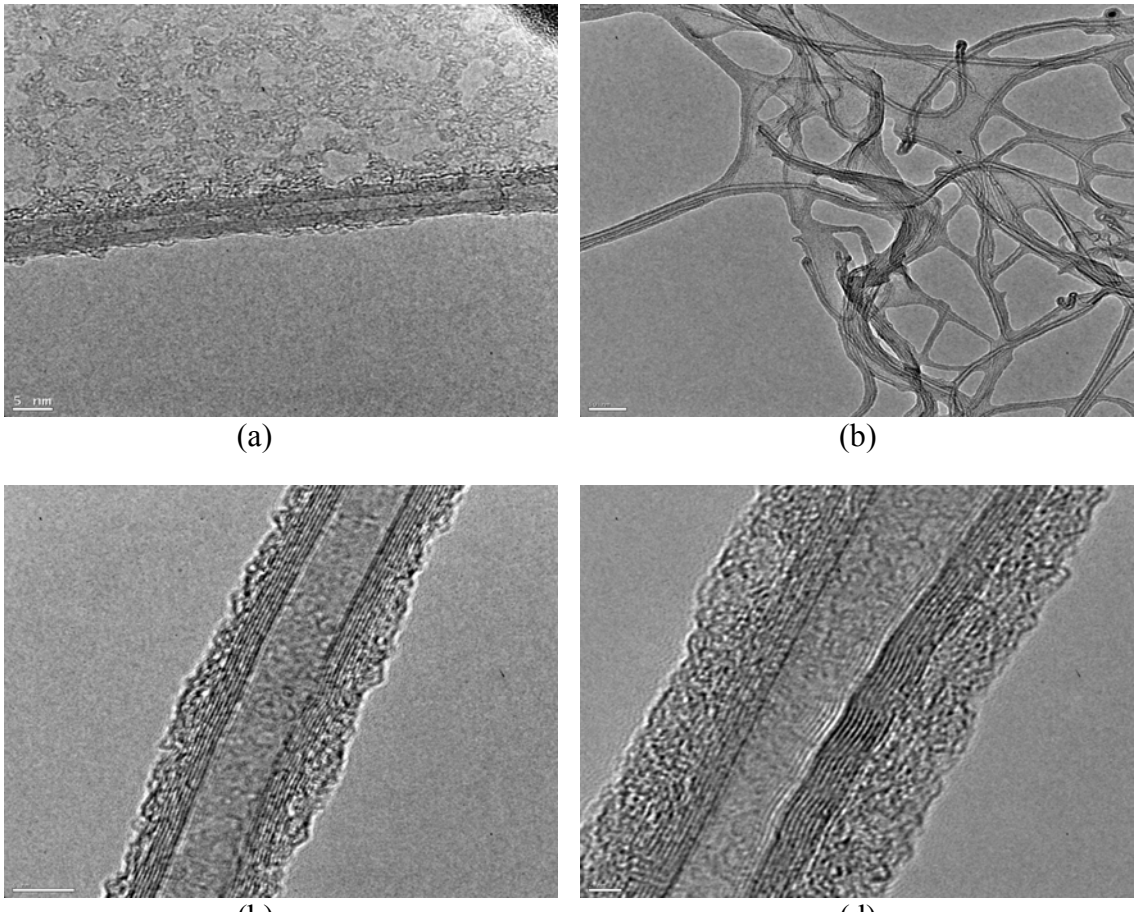

Figure 5.5. TEM micrographs of (a) CNT 513 (b) CNT 527 (c) CNT 528 (d) CNT 529

Raman spectra of sample CNT 513 produced under pure H_2 atmosphere for both pretreatment and growth atmosphere, were taken with different excitation wavelenghts and shown in Figure 5.6. Radial Breathing Mode (RBM) in the wavenumber range of 100-300 cm^{-1} is a typical feature of SWNTs and the intensity of RBM peaks of CNT 513 indicated that high amount of SWNT occured with high purity. G-band about 1590 cm^{-1} corresponds to in-plane ossilation of carbon atoms in sp^2 graphite sheet of SWNT and D-band corresponds to the disorder features of graphite sheet, therefore the low intensity of D-band relative to the G-band fort his sample indicated a very low defect density of sample.

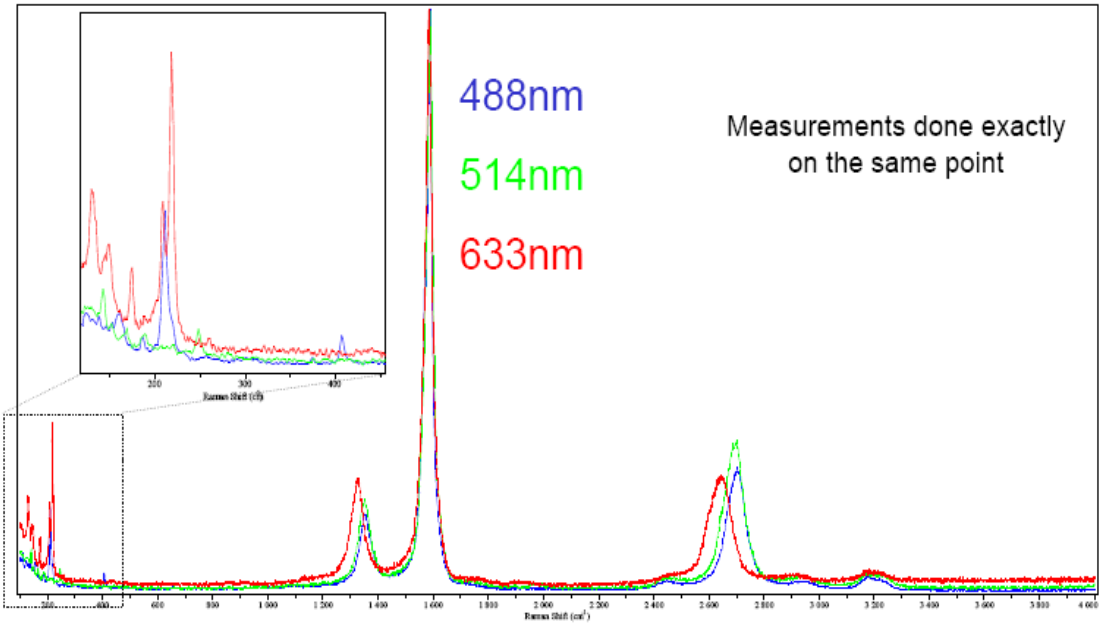

Figure 5.6. Raman spectra of CNT 513 obtained three different energies. Inset show the detailed spectra where RBM occurs.

SEM, TGA, TEM and Raman analysis all showed that hydrogen had a significant positive effect on CNT quality; high purity and yield of SWNTs were obtained under pure hydrogen atmosphere.

5.2.1.2. CNT Growth under H_2 Rich Condition

In this part of the study hydrogen and argon were flown together with methane during growth with the growth conditions of CH_4=20 sccm, H_2=20 sccm, Ar=210 sccm and T=1000 ^oC. Same four pretreatment conditions were examined for this growth condition.

Table 5.4. Examined pretreatment conditions for hydrogen lean growth condition

CNT number	Hydrogen (sccm)	Argon (sccm)
CNT 531	200	-
CNT 532	-	200
CNT 533	10	190
CNT 534	200 (for 1 h at 850 ^oC)	200 (until 850 ^oC)

SEM pictures of the as grown samples in hydrogen rich growth condition are given in Figure 5.7 for different pretreatment conditions.

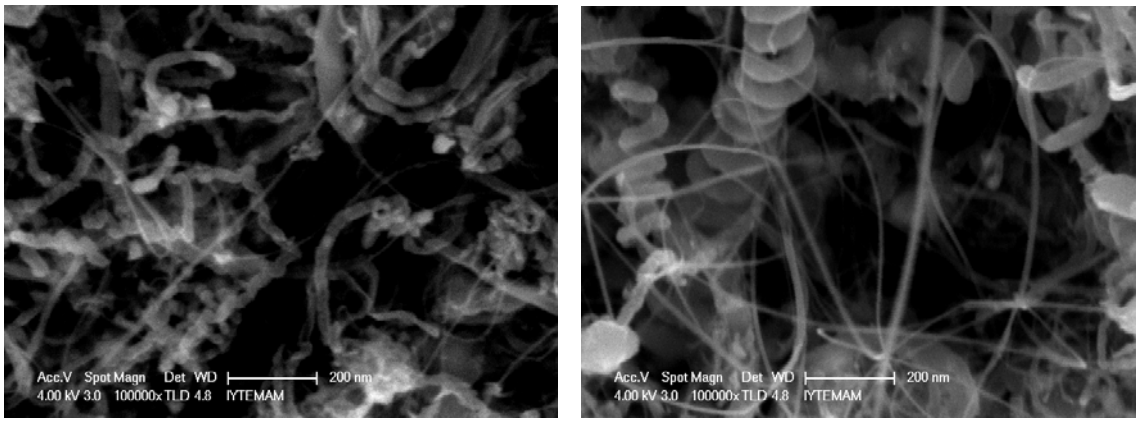

(a) (b)

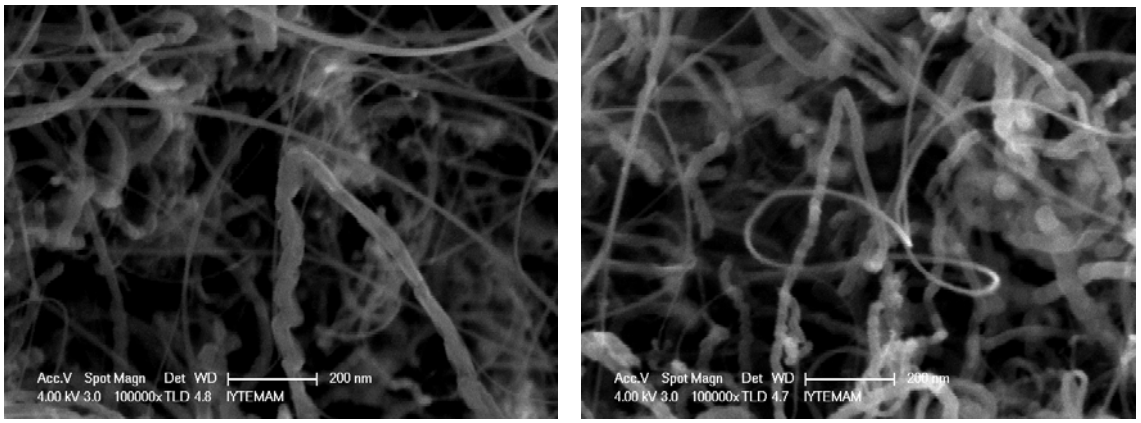

(c) (d)

Figure 5.7. SEM micrographs of (a) CNT 531 (b) CNT 532 (c) CNT 533 (d) CNT 534

For this growth condition, again CNTs with small diameters were obtained in pure hydrogen pretreatment with 9.6 nm average diameter (Table 5.4). However, this time as grown tubes did not have a high quality as can be seen from SEM images (Figure 5.7) , they were more disordered compared to the morphology of first growth with the same pretreatment conditions. In the second pretreatment process, when 200 sccm argon sent to the system for pretreatment, average diameter remained the same at 9.6 nm, but some coils, helical CNT structures were seen. As mentioned above, these coils occur in the presence of impurities. In argon and hydrogen mixture pretreatment condition, as-grown CNTs average diameter was inceased a bit. The most tangled CNTs were observed at the last pretreatment conditions, under which the thickest tubes were also obtained.

Hydrogen has a reduction effect and metal nanoparticles are more suitable than metal oxides for CNT growth. That is why the nature of product changed and the quality of CNTs decreased in hydrogen rich growth condition. Hydrogen also prevent

amorphous carbon formation, therefore when hydrogen ratio is low amorphous carbon covers CNTs and thicker tubes grow.

Table 5.5. Yield and size of CNTs for the second growth conditions

CNT number	Pretreatment	Mass Before CNT Growth (mg)	Mass After CNT Growth (mg)	Yield %	Average Diameter (nm)
CNT 531	H_2 Only	15.2	36.5	140.1	9.6
CNT 532	Ar only	15.0	21.2	41.3	9.6
CNT 533	Ar+H_2	15.1	41.5	174.8	10.9
CNT 534	H_2 for only one hour	15.1	25.4	68.2	15.8

In terms of both yield and quality the second growth conditions yielded CNTs with characteristics in general worse than the those of CNTs with first growth conditions. In these growth conditions the highest yield of product was seen in the third pretreatment process which included argon-hydrogen mixture. This time, pure hydrogen pretreatment gave 140.1% yield which is the second best in this growth condition. The other two conditions again remained under 100% yield. Especially pure argon pretreatment gave a very low yield of 41.3%.

TGA curves of as grown samples are shown in Figure 5.8. Among these four samples which give the high CNT yield is produced under pure argon pretreatment and which shows the largest weight loss step giving amorphous carbon yield is the forth sample which is produced with one hour hydrogen pretreatment. The selectivity to CNTs increases in the order of CNT 534 < CNT 531 < CNT 533 < CNT 532. However, comparing the second growth conditions to first growth conditions, all pretreatment conditions give more amourphous carbon for the second growth conditions except sample synthesized under argon-hydrogen mixture pretreatment.

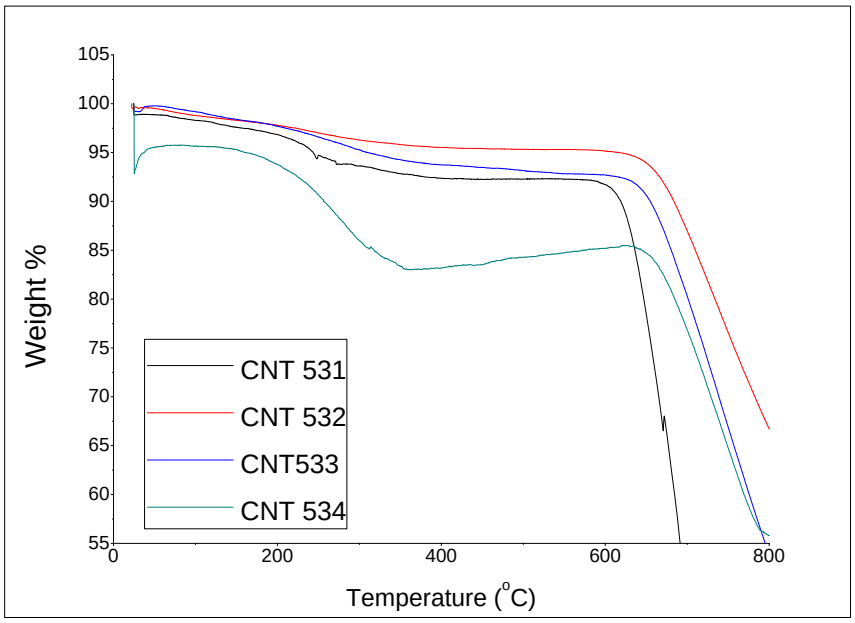

Figure 5.8. TGA diagrams of as grown samples in hydrogen rich growth condition

Table 5.6. Amorphous carbon amount of CNTs for the second growth conditions

Pretreatment	Amorphous carbon %	Transition Temp.(°C)
H_2 only	7.1	601
Ar only	4.6	626
H_2-Ar	7.1	626
Ar than H_2	12.6	649

When hydrogen ratio decreased in the growth process, number of walls increased and therefore, outer diameter also increased as depicted in figure 5.9. Again amorhous carbon were observed on the outer wall of CNTs because of growth and possibly ethanol. The first sample, CNT 531, had 18 walls; the inner and outer diameters were 2.1 nm and 14.2 nm, respectively. The second sample was CNT 532 with again 17 wall number and outer diameter was 14.2. The last one was CNT 534 which had 12 walls and it had 3.4 nm inner diameter and 10.9 nm outer diameters, respectively. TEM images showed all the carbon nanotubes grown under hydrogen rich

atmosphere were MWNTs. All MWNTs are metallic so samples grown under this atmosphere were metallic. TEM results and SEM results confirmed each other in terms of diameters of CNTs.

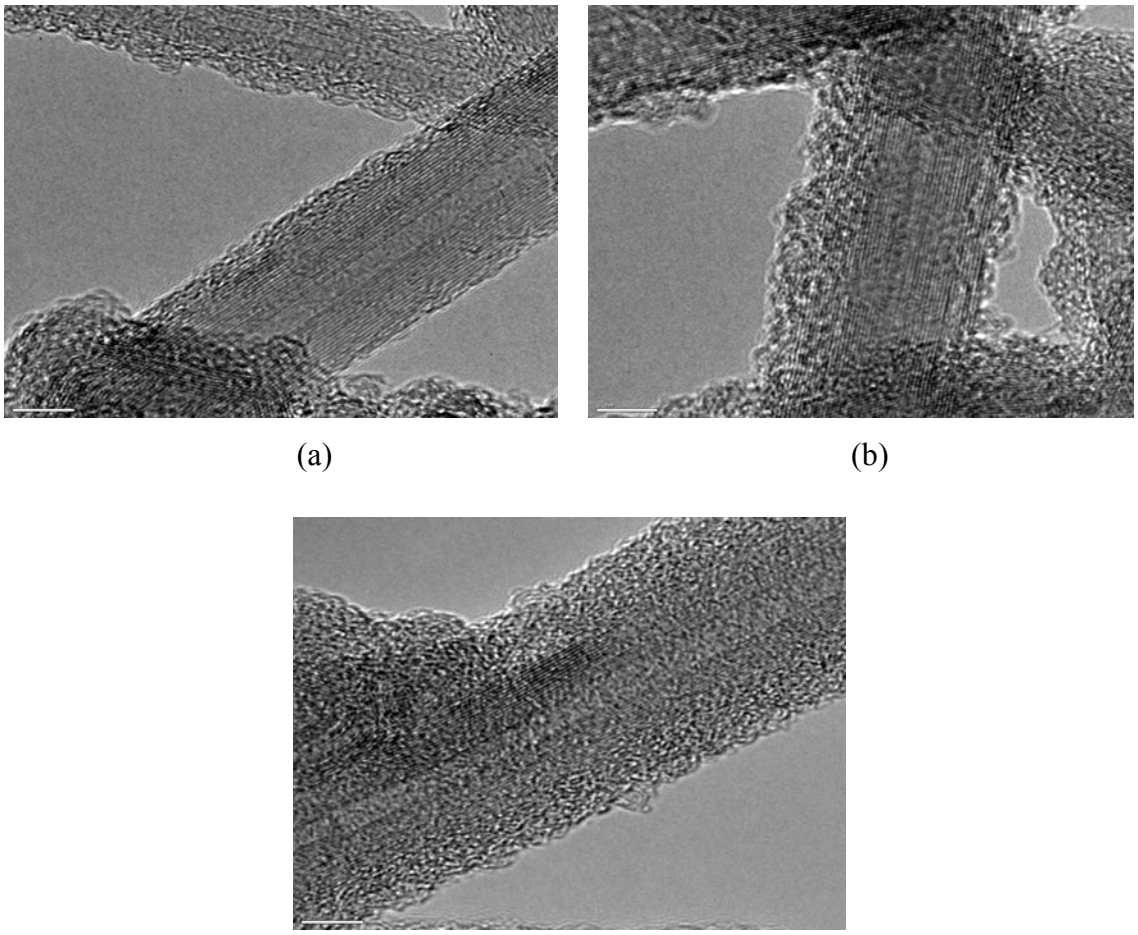

(a) (b)

(c)

Figure 5.9. TEM micrographs of (a) CNT 531 (b) CNT 532 (c) CNT 534

5.2.1.3. CNT Growth in Absence of H_2

In absence of hydrogen, only argon was flowed with methane during growth, and growth conditions were CH_4=40sccm, Ar=210sccm and T=1000^oC. Applied pretreatment conditions were given in Table 5.7.

Table 5.7. Examined pretreatment conditions for the absence of hydrogen in the growth

Sample Name	Hydrogen (sccm)	Argon (sccm)
CNT 535	200	-
CNT 536	-	200
CNT 585	10	190
CNT 601	200 (for 1h at 850 ^{o}C)	200 (until 850 ^{o}C)

SEM pictures of as grown samples at the third growth conditions are given in Figure 5.10 for these four different pretreatment conditions.

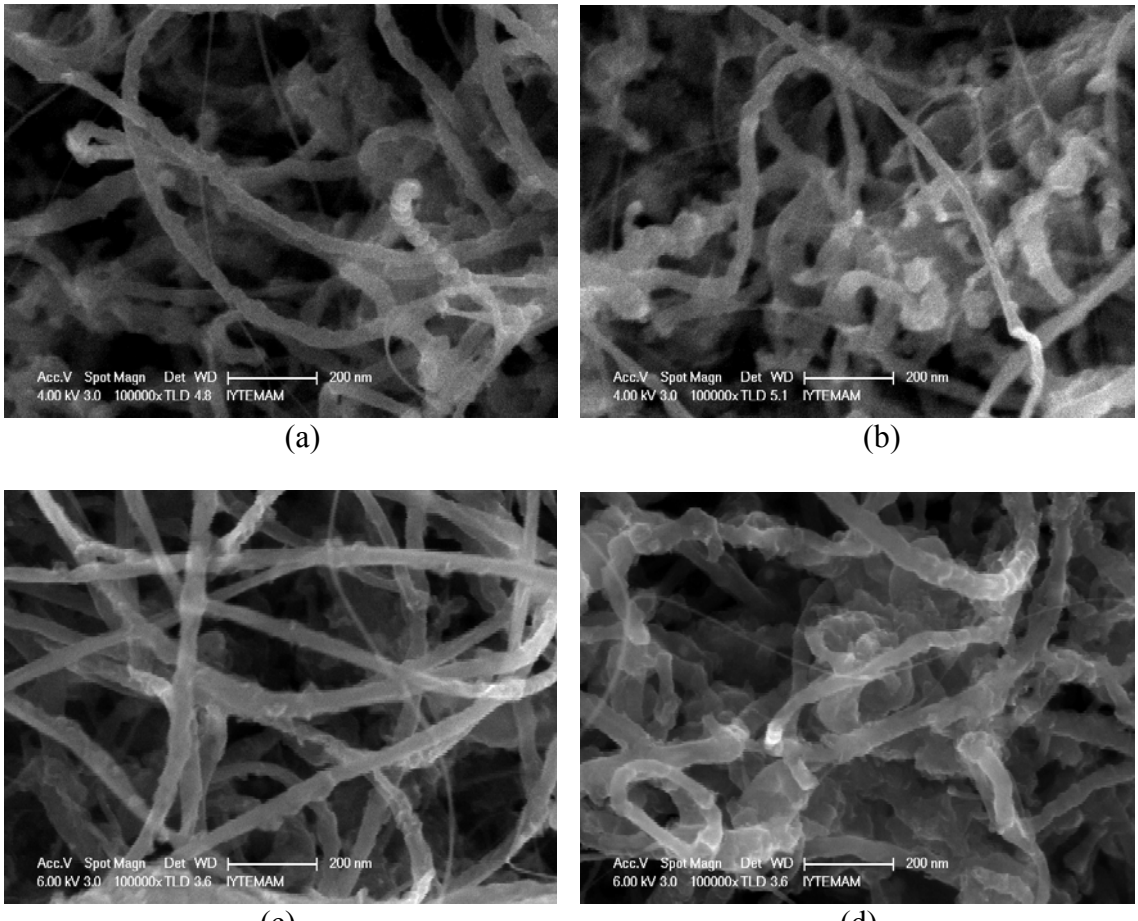

(a) (b)

(c) (d)

Figure 5.10. SEM micrographs of (a) CNT 535 (b) CNT 536 (c) CNT 585 (d) CNT 601

This time CNT structural quality was higher than hydrogen lean growth condition (H_2+Ar), but lower than the hydrogen only growth condition. They were not much disordered, but the highest CNT diameters were seen at this step. For the absence of hydrogen in growth, the thickest CNTs were obtained in argon-hydrogen mixture pretreatment with 27.0 nm average diameter while the thinnest ones occured in pure argon pretreatment with 19.2 nm. In this growth condition, at the second and forth pretreatment process amorphous carbon formation on tubes were observed and more disordered structures were also seen at these two pretreatment conditions.

Table 5.8. Yield and size of CNTs for the third growth conditions

CNT number	Pretreatment	Mass Before CNT Growth (mg)	Mass After CNT Growth (mg)	Yield %	Average Diameter (nm)
CNT 535	H_2 Only	15.1	67.8	349.0	22.5
CNT 536	Ar only	15.4	-	-	19.2
CNT 585	Ar+H_2	14.8	50.0	237.8	27.1
CNT 601	H_2 for only 1h.	15.0	70.3	368.6	26.0

The highest yield of product were observed in tests performed in absence of hydrogen. However the reason of these large numbers could be amorphous carbon formation. In these growth conditions the highest yield of product was obtained surprisingly in the forth pretreatment condition with 368.6 % yield and pure hydrogen pretreatment growth process also gave high yield, 349 %. The other two conditions again remained under 100 % yield. But, this time in all conditions yields were very high.

TGA curves of as grown samples in the third growth conditions are shown in figure 5.11. All CNTs grown with the same pretreatment conditions show a loss step between 200-500 ^{o}C. However, the largest step is seen at the forth sample which produced under only one hour hydrogen pretreatment, and this weight loss is 7.7 %. It means that none of the four samples includes very much amorphous carbon yield. TGA analysis suggests that considering also the amorphous carbon among CNTs, the increase in the diameters in SEM pictures cannot be ascribed to amorphous carbon coating of

CNTs. All samples show high crystallinity. The selectivity to CNTs increases in the order of CNT 601 < CNT 536 < CNT 535 < CNT 585 in third growth conditions.

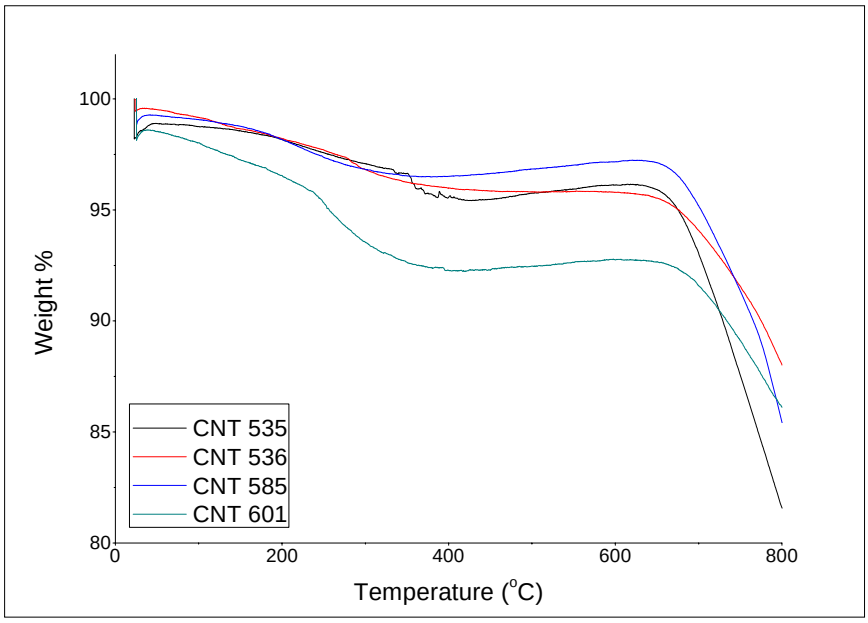

Figure 5.11. TGA diagrams of as grown samples in the third growth conditions

Raman results showed that highest graphitization was obtained for only one hour H_2 pretreatment and disorder level was higher when Ar took place in the pretreatment process.

Table 5.9. Amorphous carbon amount and Raman I_D/I_G Ratio of CNTs for the third growth conditions

Pretreatment	Amorphous carbon %	Transition Temp.(°C)	Raman I_D/I_G Ratio
H_2 only	3.3	664	0.51
Ar only	3.9	648	0.74
H_2-Ar	2.5	668	0.74
Ar than H_2	5.8	642	0.42

Now, all growth conditions can be compared using SEM and TGA datas. The highest quality CNTs were sythesized under pure hydrogen atmosphere for both pretreatment and growth processes. In the absence of hydrogen in growth, namely under argon atmosphere growth the largest diameter CNTs were obtained, but these were not tangled and so much amorphous carbon formation did not occur under these conditions. It was clearly seen that the worst growth conditions was hydrogen lean growth condition. The most tangled CNTs and amorphous carbon formation were observed here. It means when argon and hydrogen mixed together during growth, it effects negatively CNTs quality.

CNTs obtained in the absence of hydrogen in growth process were also MWNTs. CNT 536 which was produced under pure argon atmosphere in both growth and pretreatment processes is shown in figure 5.12 (b) and this image shows that very small tubes grew when there was no hydrogen in the growth ambient. This tube had 16 walls with 1.82 nm inner diameter and 12.7 nm in outer diameter.

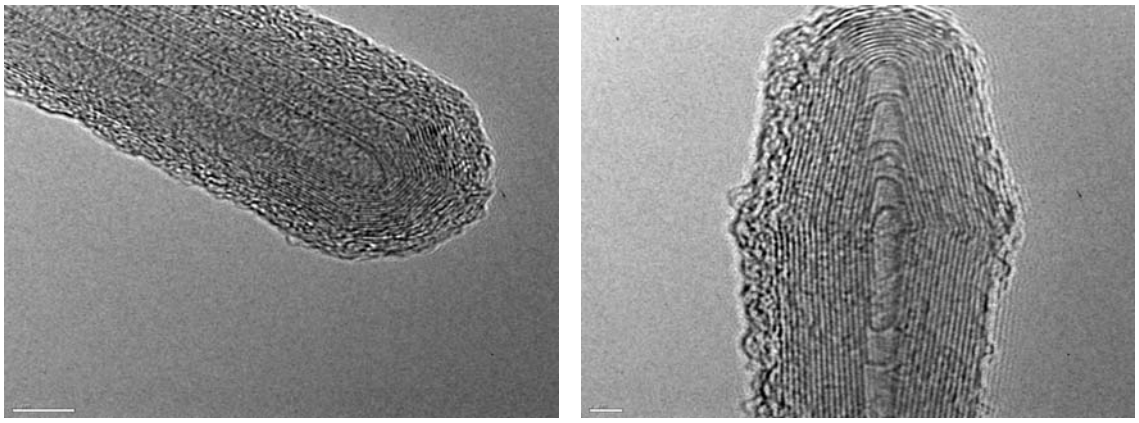

(a) (b)

Figure 5.12. TEM micrographs of (a) CNT 535 (b) CNT 536 (c) CNT 585 (d) CNT 601

(cont. on next page)

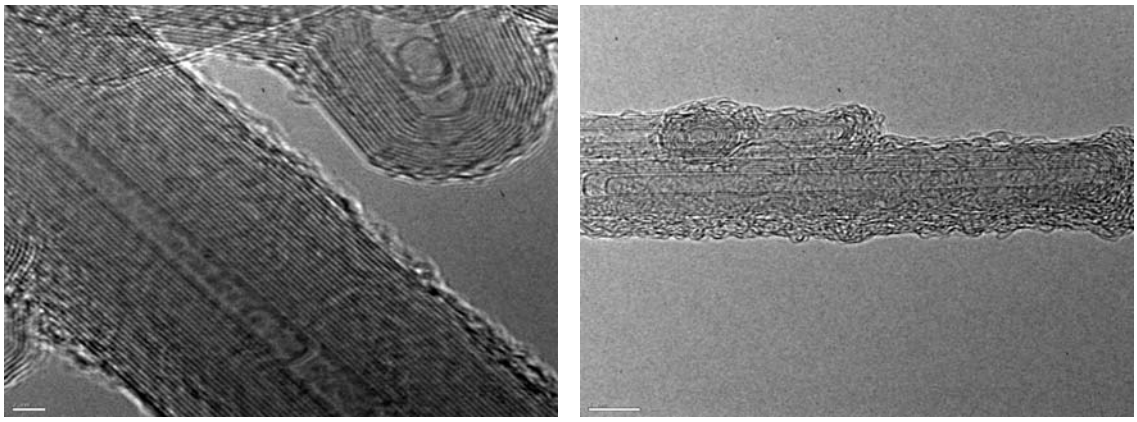

(b) (d)

Figure 5.9. (cont.)

In literature there are many studies about gas composition in CNT growth. Li *et al*. compared N_2 and H_2 atmosphere for CNT growth (Li, et al. 2004) and they did not see any difference between CNTs obtained in H_2 and N_2 atmosphere. They obtained high quaility SWNTs for both processes. However, Yu at al. compared N_2 and Ar atmosphere (Yu, et al. 2006) and their results showed that N_2 caused formation of N-doped carbon nanofibers, they could not obtain any SWNT in N_2 atmosphere, it means N_2 is active in methane decomposition. In argon atmosphere, they were able to synthesize SWNTs. In this study, SWNTs could be obtained in H_2 atmosphere, as grown samples in Ar atmosphere were all MWNTs. The reason for this difference observed with the Ar atmosphere in our results and those of Yu *et al*. are probably due to different growth conditions and catalyst material. In addition, in this study it was observed that H_2 atmosphere for both pretreatment and growth processes provided the best atmosphere to obtain high quality CNTs. H_2 reduction presentedan ideal environment for high quality growth.

5.2.2. CNT Formation at Different Hydrogen Flow Rates

The most important role of hydrogen is to prevent amorhous carbon formation by etching away amorph carbon formation during CNT growth. Hydrogen can also change the surface morphology of the catalyst during pretreatment process (Baker, et al.1982). Hence, hydrogen flow rate is a crucial parameter for the CNT growth.

During pretreatment and growth atmosphere composition study, it was seen that the pure hydrogen atmosphere yielded the highest quality CNT growth. Therefore, in this part of study, three different H_2 flow rates were investigated: 200, 150 and 100 sccm at growth temperature of 1000 ^oC for growth time of 40 min. The following table shows the flow rates of hydrogen.

Table 5.10. Examined hydrogen flow rates at the growth temperature of 1000 ^oC

CNT number	Temperature (^oC)	Hydrogen (sccm)
CNT 513	1000	200
CNT 518	1000	150
CNT 523	1000	100

SEM pictures of these as grown samples at different hydrogen flow rates are given in Figure 5.13.

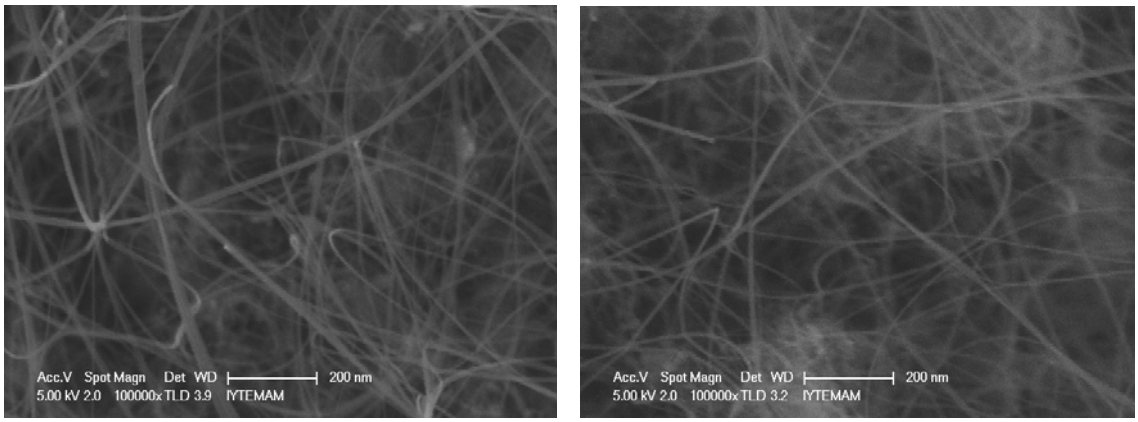

(a) (b)

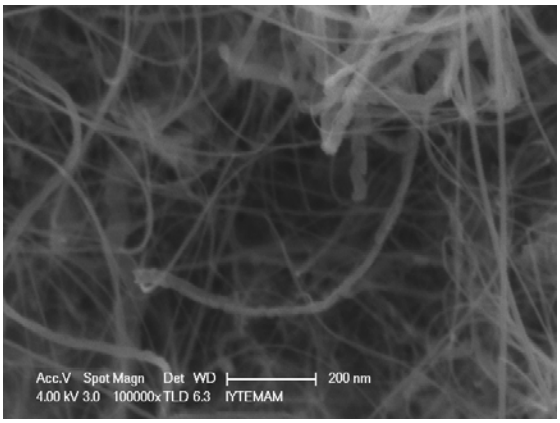

(c)

Figure 5.13. SEM micrographs of (a) CNT 513 (b) CNT 518 (c) CNT 523

It is clearly observed from SEM pictures that all CNTs grown under hydrogen atmosphere were of high quality. However, some tangled tubes were seen with decreasing hydrogen rate and it was observed that with decreasing hydrogen rate CNT areal density increased. In terms of tube diameter, samples studied do not show a large difference. All diameters were about 8.5 nm (Table 5.11).

Table 5.11. Yield and size of CNTs for different hydrogen flow rates

Hydrogen Flow Rate (sccm)	Mass Before CNT Growth (mg)	Mass After CNT Growth (mg)	Yield %	Average Diameter (nm)
200	50.2 mg	197 mg	292.4	8.3
150	50.2 mg	220.4 mg	339.04	8.5
100	29.9 mg	153.3 mg	412.71	8.5

In terms of yield, the sample produced under 100 sccm hydrogen flow rate gave the highest yield. Decreasing hydrogen flow rate resulted in increase in the yield. Comparing 100 sccm and 200 sccm hydrogen flow rates, the yield decreased about 1.5 fold. But, as seen from SEM pictures, the structural quality is directly proportional with the increasing hydrogen flow rate. Therefore, we can say that the optimum hydrogen flow rate is 150-200 sccm. This rate gave both high quality and high yield of product.

TGA curves of as grown samples in different hydrogen flow rates are shown in Figure 5.14. Almost there is no weight lost step between 200-500 ^{o}C for all three samples. However, the sample which shows highest crystallinity is produced under 200 sccm hydrogen flow. The selectivity to CNTs increases in the order of CNT 523 < CNT 518 < CNT 513. The weight loss for CNT 513 is only 3.8%. CNTs SEM and TGA analysis support each other, 200 sccm hydrogen flow is optimum for CNT growth on Co-Mo/MgO catalyst.

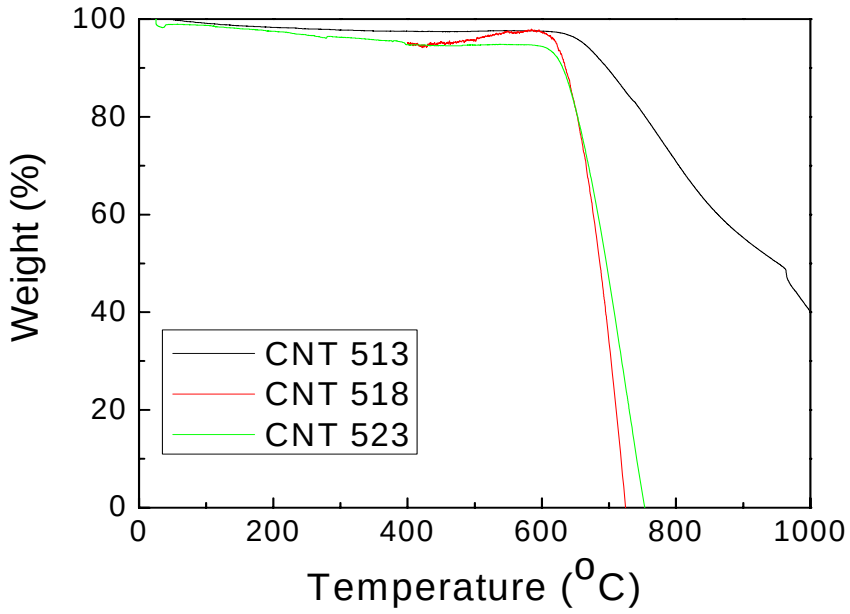

Figure 5.14. TGA diagrams of as grown samples at different hydrogen flow rates

Transition temperatures and amorphous carbon ratio showed that highest graphitization occurred for high H_2 flow rates.

Table 5.12. Amorphous carbon amount of CNTs for different hydrogen flow rates

H_2 flow rate	Amorphous carbon %	Transition Temp. (^oC)
200	0.6	649
150	2.7	602
100	5.1	612

5.2.3. CNT Formation at Different Growth Temperatures

In this part, we studied the temperature effect to find optimum CNT growth temperature. Based upon the results on the growth and pretreatment atmosphere composition and hydrogen flow rate studies results, all experiments in this part were done under 200 sccm hydrogen atmosphere. Four different temperatures were investigeted; 850 ^oC, 900 ^oC, 950 ^oC and 1000 ^oC.

Table 5.13. Examined CNT growth temperatures at 200 sccm H_2 during growth

CNT number	Temperature (^oC)	Hydrogen (sccm)
CNT 513	1000	200
CNT 524	850	200
CNT 525	900	200
CNT 526	950	200

SEM pictures of as grown samples grown at different temperatures are show in Figure 5.15.

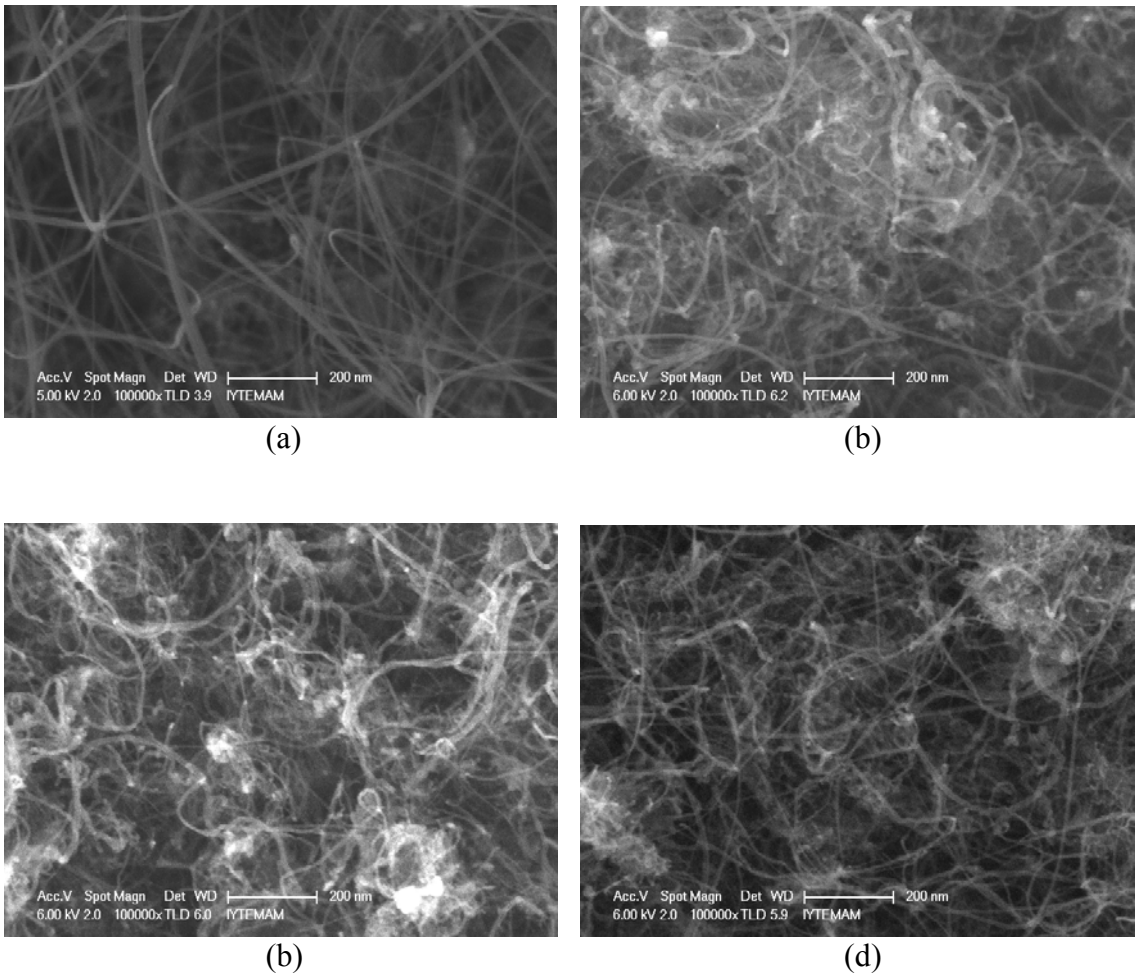

(a) (b)

(b) (d)

Figure 5.15. SEM micrographs of samples studied at different growth temperatures (a) 1000 ^{o}C (b) 850 ^{o}C (c) 900 ^{o}C (d) 950 ^{o}C

SEM pictures shows that growth temperature is a significant parameter on CNT quality. It was observed that with decreasing growth temperatures, structural quality has also decreased and CNTs became tangled. In addition, average CNT diameter also decreases with decreasing temperature and very thin tubes are obtained; while the average tube diameter was 8.3 nm at 1000 ^{o}C growth temperatures, average diameter decreases about 3 nm at low growth temperatures to about 5.7 nm.

Table 5.14. Yield, and average diameters of CNTs grown at 200 sccm H_2 for different CNT growth temperatures

Temperature (^oC)	Mass Before CNT Growth (mg)	Mass After CNT Growth (mg)	Yield %	Average Diameter (nm)
850	30.0	288.6	862.0	5.9
900	15.0	189.0	1160.0	5.7
950	15.9	264.4	1562.89	5.9
1000	50.2	197.0	292.4	8.3

Contrary to quality decreasing quality, yield increased at tempertures below 1000 ^oC. Comparing yield obtained at 1000 ^oC with those at the lower growth temparatures, yield of product increased at least 4 fold. It was observed that there was an optimum temperature to obtain highest yield and it was 950 ^oC. Below this temperature, the yield decreased. The reason for the low yield at high temperature can be explained by the behaviour of the catalyst with the temperature. Highly reactive conditions occured at very high temperature; above 950 ^oC the catalyst was deactivated before all metal particles were completely reduced. Therefore, lost of catalytic activity occured at very high temperatures and the yield was very low compared to the lower growth temperatures. Below 1000 ^oC the number of reduced catalsyt particles increased with increasing temperature, which might increases yield with inceasing temperature. Another factor was the hydrocarbon used; methane which is stable till very high temperatures and does not decompose at low temperatures. Finally, it should be emphasized that the yield obtained from growth temperature study was unprecedently high compared to the current literature.

TGA curves of as grown samples at growth different temperatures are given in Figure 5.16. The quality of CNTs in terms of less amorphous carbon content increases in the order of CNT 524 < CNT 525 < CNT 526 < CNT 513. CNT 513, CNT 525 and CNT 526 showed similar TGA curves with temperature. Only CNT 524 which was synthesized at 850 ^oC showed a distinct weight loss step. Generally, it can be said that amorphous carbon formation decreases with increasing temperature. The observed behaviour can be explained by that at low temperature there were not enough reduced

catalytic sites and carbon which was obtained from decomposition of methane can not precipitate on the catalyst particles, so to form amorphous carbon.

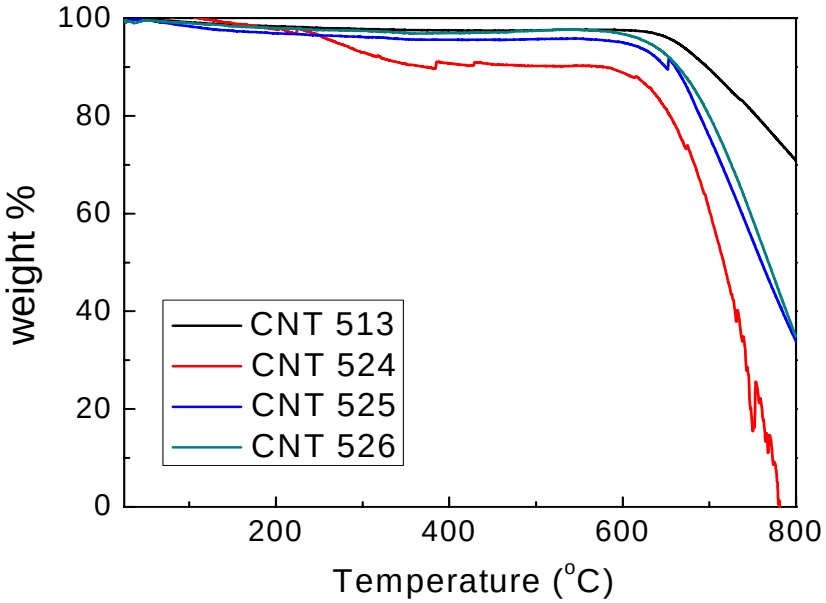

Figure 5.16. TGA diagrams of as grown samples at different growth temperatures

Raman spectra I_D/I_G ratio supported TGA and SEM datas disorder level decreased with increasing temperature.

Table 5.15. Amorphous carbon amount and Raman I_D/I_G Ratio of CNTs for different growth temperatures

Growth Temperature (°C)	Amorphous carbon %	Transition Temperature (°C)	Raman I_D/I_G Ratio
850	10.1	613	0.91
900	3.6	607	0.29
950	3.1	625	0.19
1000	0.6	649	0.16

In this study, the first target was to synthesize high quality CNTs. So, despite of very high yield CNT formation at lower temperatures, the best growth temperature for high structured quality CNT growth was designated as 1000 ^{o}C.

In literature Kang et al. studied temperature effect on CNT growth using Fe-Mo/MgO catalyst (Kang, et al. 2008) and their results were different. They studied 800, 850, 900 and 1000 ^{o}C growth temperatures and with increasing temperatures they observed amorphous carbon coating on CNTs and DWNT ratio to SWNT also increased with temperature and it depended on the agglomeration of catalyst particle in relatively high temperature. Our results were different because of catalyst effect. While Fe-Mo/MgO catalyst agglomerating at high temperatures, Co-Mo/MgO catalyst might have not do the same.

5.2.4. CNT Formation at Different Growth Times

Growth time is also considered as an important parameter in CNT synthesis and in the last part of this study we examined the growth time effect on CNT growth in order to understand growth mechanism of CNTs. Five different growth times were investigated; 10, 20, 30 and 40 minutes. All growth time study took place under 200 sccm hydrogen and 50 sccm methane flow, at 1000 ^{o}C.

Table 5.16. Examined growth times for CNT growth under 200 sccm H_2 50 sccm CH_4 at 1000 ^{o}C

CNT number	Time (min.)	Hydrogen (sccm)
CNT 513	40	200
CNT 606	30	200
CNT 609	20	200
CNT 615	10	200

SEM pictures of as grown samples at different growth times are given in Figure 5.17.

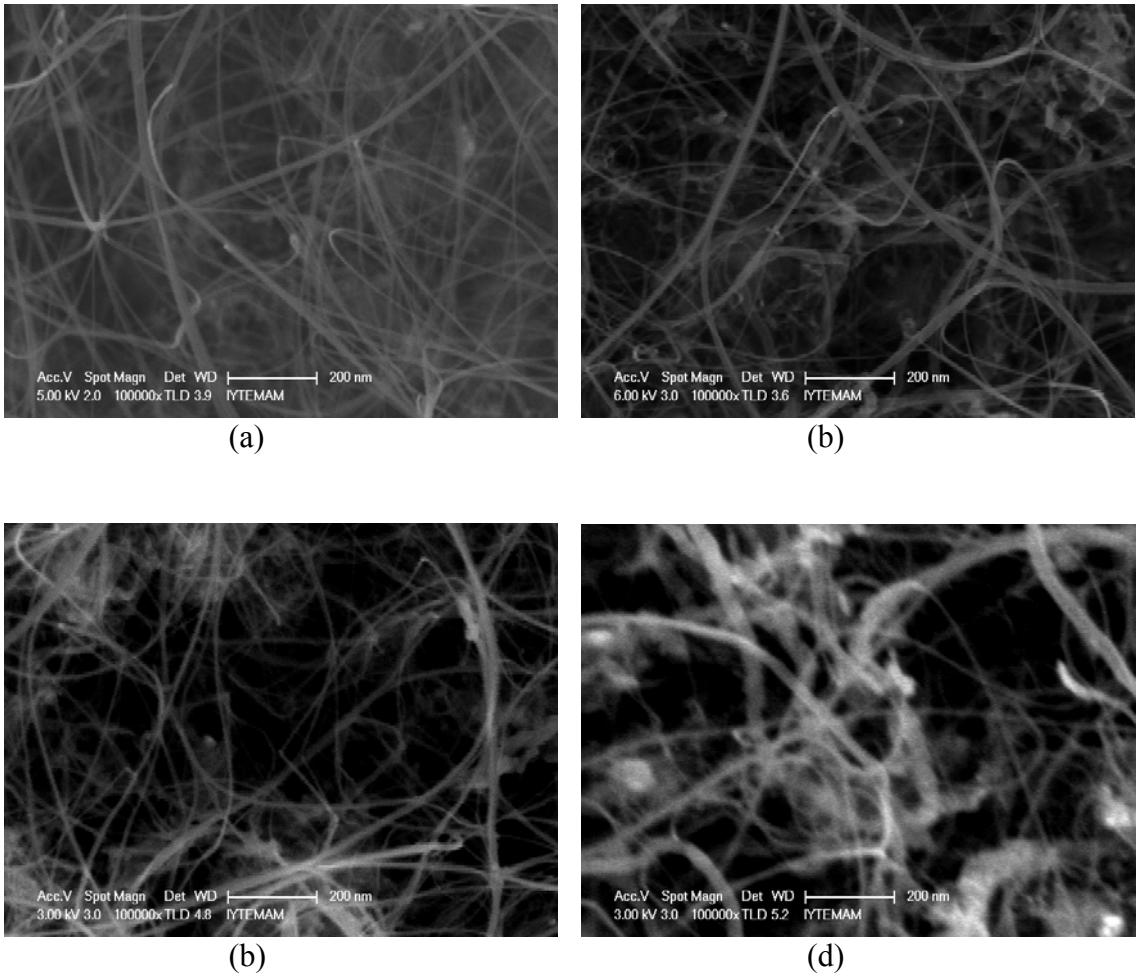

Figure 5.17. SEM micrographs of growth for (a) 40 min. (b) CNT 30 min. (c) 20 min. (d) 10 min.

SEM pictures of CNTs grown at different growth times pointed that the density of CNTs increases with time. CNTs became longer and graphitization was higher at longer growth times. Disorder also decreases with increasing time. It was seen that there were catalyst particles remaining on the surface at 10 min and 20 min growth and methane decomposition was still assumed taking place, but at 40 min no more catalytic sites were observed and highly ordered tubes were obtained.

Table 5.17. Yield and size of CNTs for different CNT growth times

Time	Mass Before CNT Growth (mg)	Mass After CNT Growth (mg)	Yield %	Average Diameter (nm)
40	50.2	197.0	292.4	8.3
30	14.9	65.4	338.9	7.8
20	15.1	65.2	331.7	8.8
10	15.3	45.1	194.7	14.1

Yield also increased with time, similar to structural quality improved as observed from SEM study. However, yield was above 100 % even at 10 min growth time. Although the yield increased continuously in time till 30 minutes, the increasing ratio decreased (Figure 5.18). However, after 30 minutes of growth time yield stated to decrease.

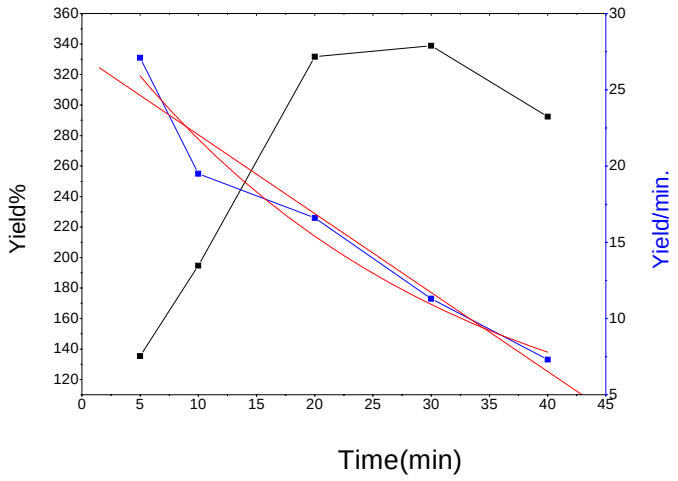

Figure 5.18. Yield% -Time graph.

Table 5.18. Raman I_D/I_G Ratio of CNTs for different growth times

Time (min.)	Raman I_D/I_G Ratio
40	0.16
30	0.20
20	0.23
10	0.28

As seen from Raman results graphitization increased with increaseing time. Niu *et al*. also studied growth time effect on CNT growth using Fe-Mo/MgO catalyst (Niu, et al. 2006) and their results were similar to our results. CNTs lenght and yield increased with time also in their study. In conslusion, the best growth time was found as 30-40 min for high quality of product.

CHAPTER 6

CONCLUSIONS

In this work, the aim was to grow high quality and large scale of carbon nanotubes on Co-Mo/MgO catalyst. Different growth parameters were studied and the optimum CNT growth conditions were investigated. CNT growth and pretreatment atmosphere composition, hydrogen flow, growth temperature and lastly growth time effects on CNTs were examined to optimize parameters. Then CNTs were characterized structurally.

In the first part, gas composition effect during both growth and catalyst pretreatment processes was examined for three different growth condition and four different pretreatment conditions for each growth condition and used gases were argon and hydrogen. This study showed that hydrogen gas was necessary for both pretreatment and growth atmosphere for high quality growth. It reduced catalsyt particles during pretreatment and prevented other carboneaous product formation during growth. Therefore hydrogen provided clean and high quality CNTs formation.

In the second part of study, 200, 150 and 100 sccm H_2 flow rates were examined. And it was seen that some disorder started to seem with decreasing hydrogen rate and an increase in the density of CNTs occured with decreasing hydrogen rate.

Then, the temperature effect was investigated for four different temperature value, 850 ^{o}C, 900 ^{o}C, 950 ^{o}C, 1000 ^{o}C. Temperature study showed that CNTs quality increased with increasing tempertaure. However, the results for yield was different. It was seen that 950 ^{o}C was optimum temperature to obtain high yield, below this temperature the yield decreased. We saw that above 950 ^{o}C, the catalyst deactivated before all metal particles were completely reduced and the yield could not increase, and below 950 ^{o}C the reduced catalsyt particles increased with increasing temperature and so the yield increased with inceasing temperature. The maximum obtained yield was above 1500 % and average diameter was about 5 nm in this study.

Growth time was the last parameter studied in this thesis work. To understand growth time effect on CNT growth five different growth time were investigated fort his part, these were 5, 10, 20, 30 and 40 minutes. According to results, the density and the

length of CNTs increased with time. The amount of tangled CNTs decreased with growth time. Catalyst particles were observed on the surface at 10 min and 20 min growth. At 40 min highly ordered tubes were grown. Yield also increased with time similar to quality.

As a conclusion, the best atmosphere for methane decomposition on Co-Mo/MgO catalyst was hydrogen atmosphere because hydrogen provides transformation metal oxides to metals and metals are suitable materials for CNT growth and for high quality CNT synthesis the best hydrogen flow rate is 200 sccm. Moreover, from the temperature study results we can say that high temperature is appropriate for methane decomposition, so the ideal growth temperature is found as 1000 ^{o}C at this study. Finally, for high qulity and long tubes enough growth time is 40 minutes.

REFERENCES

Ago, H., N. Uehara, N. Yoshihara, M. Tsuji, M. Yumura, N. Tomonaga, T. Setoguchi. 2006. Gas analysis of the CVD process for high yield growth of carbon nanotubes over metal-supported catalysts. Carbon 44: 2912-2918.

Armor, J.N., E. J. Carlson. A Novel Procedure for "Pelletizing" Aerogels.1985. Appl. Catal. 19:327–337.

Arthur, J. and A. Cho. 1973. Adsorption and desorption kinetics of Cu and Au on (0001) graphite. Surface Science 36:64-660.

Baddour, C. and C. Briens. 2005. Carbon Nanotube Synthesis : a review R3.Internation Journal of Chemical Reactor Engineering 3 :20-22.

Belin T., Epron F. 2005. Characterization methods of carbon nanotubes. Materials Science and Engineering B. 119: 105–118.

Biris, A.R., Z. Li, E. Dervishi, D. Lupu, Y. Xu, V. Saini, F. Watanabe, A.S. Biris. 2008. Effect of hydrogen on the growth and morphology of single wall carbon nanotubes synthesized on a Fe-Mo/MgO catalytic system. Phys. Letters A.

Bonadiman, R., M.D. Lima, M.J. Andrade, C.P. Bergmann. 2006. Production of single and multi walled carbon nanotubes using natural gas as a precursor compound. J. Mater. Sci. 41:7288-7295.

Breitscheidel, B., J. Zieder, U. Schubert. 1991. Metal Complexes in Inorganic Matrices. 7. Nanometer-Sized, Uniform Metal Particles in a SiO2 Matrix by Sol-Gel Processing of Metal Complexes. Chem. Mater. 3: 559–566.

Brinker, C.J., K. D. Keefer, D. W. Schaefer, C. S. Ashley. 1982. Sol-Gel Transition in Simple Silicates. J. Non-Cryst. Solids, 48: 47–64.

Chai, S.P., S.H.S. Zain, A.R. Mohamed. 2006. Preparation of carbon nanotubes over colbalt-containing catalysts via catalytic decomposition of methane. Chem. Phys. Letters 426:345-350.

Cui, H., G. Eres, J.Y. Hawe. 2003. Growth behavior of carbon nanotubes on multilayered metal catalyst film in CVD. Chemical Physics Letters 374 : 222-228.

Daenen, M., R.D. de Fouw, B. Hamers, P.G.A. Janssen, K. Schouteden, M.A.J. Veld. 2003.The Wondrous World of Carbon Nanotubes. Eindhoven University of Technology.

Dai H. 2002. Carbon nanotubes: opportunities and challenges. Surface Science 500:218-241.

Deck, C.P. and K. Vecchio. 2006. Prediction of Carbon nanotube growth success by the analysis of carbon-catalyst binary phase diagrams. Carbon 44:267-275.

Deschler, U., P. Kleinschmit, P. Panster. 1986. 3-Chloropropyltrialkoxysilanes-Key Intermediates for the Commercial Production of Organofunctionalized Silanes and Polysiloxanes. Angew. Chem. Int. Ed. Engl. 25: 236–252.

Dresselhaus, Mildred S., Gene Dresselhaus, and Phaedon Avouris, eds. 2001. Carbon nanotubes: synthesis, structure, properties, and applications. Berlin: Springer Publishers.

Dresselhaus, M.S., G. Dresselhaus, A. Jorio, A.G.S. Filho, and R. Saito. 2002. Raman Spectroscopy on isolated single wall carbon nanotubes. Carbon 40:2043-2061.

Dresselhaus, M.S., Y. M. Lin, O. Rabin, A. Jorio, A.G. Souza, M.A. Pimenta, R. Saito, G.G.Samsonidze, and G. Dresselhaus. 2003.Nanowires and nanotubes.Materials Science and Engineering C 23(1-2):129-140.

Dupuis, A.C. 2005. The catalyst in the CCVD of carbon nanotubes: a review. Progress in Materials Science 50(8):929-961.

Ebbesen, T.W. 1993. Carbon nanotube. Annual Review Matterials 24:235-264.

Flahaut, E., C. Laurent, A. Peigney. 2005. Catalytic CVD synthesis of double and triple-walled carbon nanotubes by the control of the catalyst preparation. Carbon 43: 375–383.

Fonseca, A., K. Hernadi, J.B. Nagy, D. Bernaerts, and A.A. Lucas. 1996. Optimization of catalytic production and purification of buckytubes. Journal of Molecular Catalysis A: Chemical 107:159-168.

Guo, T., P. Nikolaev, A. Thess, D.T. Colbert, and R.E. Smalley. 1995. Catalytic growth of single-walled nanotubes by laser vaporization. Chemical Physics Letters 243:49-54.

Guo, T, P. Nikolaev, A.G. Rinzler, D. Tomanek, D. T. Colbert, and R.E, Smalley. 1995. Self-assembly of tubular fullerenes. Journal of Physical Chemistry 99(27):10694-10697.

Harris, P. J. F. 2007.Solid state growth mechanisms for carbon nanotubes.Carbon 45:229-239.

Heinrichs, B., F. Noville, J.P. Pirard. 1997. Pd/SiO2-Cogelled Aerogel Catalysts and Impregnated Aerogel and Xerogel Catalysts: Synthesis and Characterization. J. Catal. 170:366–376.

Hernadi, K., A. Fonseca, J.B. Nagy, D. Bernaerts, A. Fudala, and A.A. Lucas. 1996. Catalytic synthesis of carbon nanotubes using zeolite support. Zeolites 17:416-423.

Iijima, S. 1991. Helical microtubules of graphitic carbon. Nature 354:56-58.

Iijima, S. and T. Ichihashi. 1993. Single-shell carbon nanotubes of 1 nm diameter. Nature 363:603-605.

Ivanov, V., J. B. Nagy, P. Lambin, A. Lucas, X.F. Zhang, and D. Bernaerts. 1994. The study of carbon nanotubules produced by catalytic method. Chemical Physics Letters 223:329-335.

Ji, L., S. Tang, H. C. Zeng, J. Lin, K. L. Tan. 2001. CO_2 Reforming of Methane to Synthesis Gas over Sol-Gel-Made Co/Al_2O_3 Catalysts from Organometallic Precursors. Appl. Catal. A. 207: 247–255.

Journet, C. and P. Bernier. 1998. Production of carbon nanotubes. Applied Physics A 67:1-9.

Kathyayini, H., K.V. Reddy, J.B. Nagy, N. Nagaraju. 2008. Synthesis of carbon nanotubes over transition metal ions supported on $Al(OH)_3$. Indian J. Chem. 47A:663-668.

Kang, S.G., K.K. Cho, K.W. Kim, G.B. Cho. 2008. Catalytic growth of single and double-walled carbon nanotubes from Fe-Mo nanoparticles supported on MgO. J. Alloys and Compounds 449: 269-273.

Kiang, C., M. Endo, P. Ajayan, G. Dresselhaus, M. Dresselhaus. 1998. Size Effects in Carbon Nanotubes. Phys. Rev. Lett. 81: 1869-1872.

Ko, E.I. 1997. Sol-Gel Process, Handbook of Heterogeneous Catalysis (G. Ertl, H. Knozinger, and J. Weitkamp, Eds.), Wiley-VCH. Weinheim 86–94.

Kong, J., A.M. Cassell, H. Dai. 1998. Chemical vapor deposition of methane for single-walled carbon nanotubes. Chemical Physics Letters 292:567–574.

Kroto, H.W., J.R. Heath, S.C. O'Brien, R.F. Curl, R.E. Smalley. 1985. C60: buckminsterfullerene. Nature 318:162-163.

Kukovecz, A., Z. Konya, N. Nagaraju, I. Willems, A. Tamasi, A. Fonseca, J. B. Nagy, and I. Kiricsi. Catalytic Synthesis of Carbon Nanotubes over Co, Fe and Ni Containing Conventional and Sol-Gel Silica-Aluminas. 2000. Phys. Chem. Chem. Phys. 2: 3071–3076.

Lambert, S., C. Cellier, P. Grange, J.-P. Pirard, B. Heinrichs. 2004. Synthesis of Pd/SiO2, Ag/SiO2, and Cu/SiO2 Cogelled Xerogel Catalysts: Study of Metal Dispersion and Catalytic Activity. J. Catal. 221: 335–346.

Lee, Y., T. Cho, B. Lee, J. Rho, K. An, Y. Lee. 2003. Surface properties of fluorinated single-walled carbon nanotubes. J. Fluorine Chem 120: 99-104.

Li, Y., W. Kim, Y. Zhang, M. Rolandi, D. Wang, and H. Dai. 2001. Growth of single walled carbon nanotubes from discrete catalytic nanoparticles of various sizes. Journal of Physical Chemistry B 105:11424-11431.

Li,W.Z., D.Z. Wang, S.X.Yang, J.G.Wen. 2001. Chemical Physics Letters 335:141-149.

Li, Y., X. Zhang, L. Shen, J. Luo, X. Tao, F. Liu, G.Xu, Y. Wang, H.J. Geise, G.V. Tendeloo. 2004. Controlling the diameters in large-scale synthesis of single-walled carbon nanotubes by catalytic decomposition of CH_4. Chem. Phys. Letters 398:276-282.

Liu, B.C., S.C. Lyu, S.I. Jung, H.K. Kang, C.W. Yang, J.W. Park, C.Y. Park, C.J. Lee. 2004. Single-Walled Carbon Nanotubes Prodeced by Catalytic Chemical Vapor Deposition of Acetylene over Fe-Mo/MgO Catalyst. Chem. Phys. Letters 383: 104-108.

Liu, B.C., B. Yu, M.X. Zhang. 2005. Catalytic CVD Synthesis of double-walled carbon nanotubes with a narrow distribution of diameters over Fe-Co/MgO catalyst. Chem. Phys. Letters 407: 232-235.

Liu, Q., Y. Fang. 2006. New technique of synthesizing single-walled carbon nanotubes from ethanol using fluidized-bed over Fe-Mo/MgO catalyst. Spectrochimica Acta Part A 64:296-300.

Liu, Y., W. Wongwiriyapan, K.C. Park, H. Muramatsu, K. Takeuchi, Y.A. Kim, M. Endo. 2009. Combined catalyst system for preferential growth of few-walled carbon nanotubes. Carbon 47: 2543-2546.

Loiseau, A., J. Gavillet, F. Ducastelle, J. Thibault, O. Stephan, P. Bernier, S. Thair. 2003. Nucleation and growth of SWNT: TEM studies of the role of the catalyst. C. R. Physique 4: 975–991.

Lopez, T., A. Romero, R. Gomez. Metal-Support Interaction in Pt/SiO2 Catalysts Prepared by the Sol-Gel Method.1991. J. Non-Cryst. Solids 127: 105–113.

Maser, W., E. Munoz, A. M. Benito, M. T. Martinez, G. F. de la Fuente, Y. Maniette, E. Anglaret, J. L. Sauvajol. 1998. Production of high-density single-walled nanotube material by a simple laser-ablation method. Chemical Physics Letters 292: 587-593.

Mathieu, B., S. Blacher, R. Pirard, J.P. Pirard, B. Sahouli, F. Brouers. Freeze-Dried Resorcinol-Formaldehyde Gels. 1997. J. Non-Cryst. Solids 212: 250–261.

Mehn, D., A. Fonseca, G. Bister, J.B. Nagy. 2004. A comparison of different preparation methods of Fe-Mo/Al_2O_3 sol-gel catalyst for synthesis of single wall carbon nanotubes. Chem. Phys. Letters 393:378-384.

Moisala, A., A.G. Nasibulin, E.I. Kapauppinen. 2003. The role of metal nanoparticles in the catalytic production of single-walled carbon nanotubes. Journal of Physics: condensed matter 15:3011-3035.

Niu, Y. Fang. 2006. Effects of synthesis time for synthesizing single-walled carbon nanotubes over Mo–Fe–MgO catalyst and suggested growth mechanism. J.Crystal Growth 297: 228-233.

Ning, Y., X. Zhang, Y. Wang, Y. Sun, L. Shen, X. Yang, G.V. Tendeloo. 2002. Bulk production of multi-wall carbon nanotube bundles on sol-gel prepared catalyst. Chem. Phys. Letters 366: 555-560.

O'Connor, J. 2003. Surface analysis methods in materials science. Springer.

Pajonk, G.M. Catalytic Aerogels. 1997. Catal. Today 35: 319–337.

Paradise, M., and T. Goswami. 2007. Carbon nanotubes-production and industrial applications. Mater. & Design 28: 1477-1489.

Park J.B, G.S. Choi, Y.S. Cho, S.Y. Hong, D. Kim, S.Y. Choi, J.H. Lee, K. Cho. 2002. Characterization of Fe-catalyzed carbon nanotubes grown by thermal chemical vapor deposition. Journal of Crystal Growth 244:211-217.

Pirard, R., J.P. Pirard. Aerogel Compression Theoretical Analysis. 1997. J. Non-Cryst. Solids 212: 262–267.

Popov, V.N.2004. Carbon nanotubes: properties and applications. Materials Science and Engineering Reports 43:61-102.

Qingwen, L., Y. Hao, C. Yan, Z. Jin, L. Zhongfan. 2002. A scalable CVD synthesis of high-purity single-walled carbon nanotubes with porous MgO as support material. J. Mater. Chem. 12: 1179-1183.

Rao, A., R. Richter, S. Bandow, B. Chase, P. Eklund, K.A. Williams, S. Fang, K.R. Subbaswamy, M. Menon, A. Thess, R. Smalley, G. Dresselhaus, M. Dresselhaus. Diameter-Selective Raman Scattering from Vibrational Modes in Carbon Nanotubes. 1997. Science 275:187.

Rashidi, A.M., M.M. Akbarnejad, A.A. Khodadadi, Y. Mortazavi, A. Ahmadpourd. 2007 Single-wall carbon nanotubes synthesized using organic additives to Co-Mo catalysts supported on nanoporous MgO. Nanotechnology 18: 315605-315609.

Reich, S., C. Thomsen, and J. Maultzsch. 2004.Carbon nanotubes: basic concepts and physical properties. Berlin: Wiley-VCH.

Regalbuto, J. 2007. Catalyst preparation science and engineering. CRC Press.

Richardson, J. T. 1989. Principles and catalyst development. New York: Plenum Press.

Rotkin, Slava V. and Shekhar Subramoney, eds. 2005.Applied physics of carbon nanotubes: fundamentals of theory, optics, and transport devices. New York: Springer Publishers.

Saito, Riichiro, Gene Dresselhaus, and Mildred S. Dresselhaus. 1998. Physical properties of carbon nanotubes. London: Imperial College Press.

Salvetat, G. Andrew, D. Briggs, J.M. Bonard, Revathi, R. Bacsa, Andrzej, J. Kulik, T. Stockli, N.A. Burnham, L. Forro. 1998. Physical Review Letters 82.

Saito, R., M. Fujita, G. Dresselhaus, M.S. Dresselhaus. 1992. Electronic structure of chiral graphene tubules. Applied Physics Letters 60(18):2204-2207.

Shanov V., Y.H. Yun, M.J. Schulz. 2006. Synthesis and characterization of carbon nanotube materials. Journal of the University of Chemical Technology and Metallurgy 41(4):377-390.

Singh, C., M.S.P. Shaffer, H. Windle. 2003. Production of controlled architectures of aligned carbon nanotubes by an injection chemical vapour deposition method. Carbon 41: 359–68.

Stahl, H. 2000. Electronic Transport in Ropes of Single Wall Carbon Nanotubes. Achen University of Technology.

Schaefer, D.W., R. Pekala, G. Beaucage. Origin of Porosity in Resorcinol-Formaldehyde Aerogels. 1995. J. Non-Cryst. Solids 186: 159–167.

Schneider, M., A. Baiker. Aerogels in Catalysis. 1995. Catal. Rev.-Sci. Eng. 37: 515–556.

Su, M., B. Zheng, J. Liu. 2000. A scalable CVD method for the synthesis of single-walled carbon nanotubes with high catalyst productivity. Chem. Phys. Letters 322: 321-326.

Suh, D.J., T.J. Park, J.H. Kim, K.L. Kim. Nickel-Alumina Aerogel Catalysts Prepared by Fast Sol-Gel Synthesis.1998. J. Non-Cryst. Solids 225: 168–172.

Scott, C. D., S. Arepalli, R. Nikolaev, R. E. Smalley. 2001. Growth Mechanisms for Single-Wall Carbon Nanotubes in a Laser-Ablation Process. Applied Physics A: Materials Science & Processing 72: 573-580.

Sinnott, S. B., R. Andrews, D. Qian, A.M. Rao, Z. Mao, E.C. Dickey, F. Derbyshire. 1999. Model of carbon nanotube growth through chemical vapor deposition. Chem.Phys.Lett. 315: 25-30.

Tans, S. J., M.H. Devoret, H. Dai, A. Thess, R.E. Smalley, L.J. Geerligs, and C. Dekker. 1997. Individual single-wall carbon nanotubes as quantum wires. Nature 386:474-477.

Thess, R. Lee and R. E. Smalley. 1996. Crystalline Ropes of Metallic Carbon Nanotubes. Science 273: 483.

Tran, K.Y., B. Heinrichs, J.F. Colomer, J.P. Pirard, S. Lambert. 2007. Carbon nanotubes synthesis by the ethylene chemical catalytic vapour deposition (CCVD) process on Fe, Co, and Fe-Co/Al_2O_3 sol-gel catalysts. Applied Catalysis A 318:63-69.

Venegoni, D., P. Serp, R. Feurer, Y. Kihn, C. Vahlas, and P. Kalck. 2002. Parametric study for the growth of carbon nanotubes by catalytic chemical vapor deposition on a fluidized bed reactor Carbon 40:1799-1807.

Walker, P.L., F. Rusinko, L.G. Austin. 1959. Gas reactions of carbon. Advances in Catalysis 11:133-221.

Ward, D.A., E. I. Ko. Preparing Catalytic Materials by the Sol-Gel Method. 1995. Ind. Eng. Chem. Res. 34: 421–33.

Weifeng, L., W. Cai, L.Yao, X. Li, Z. Yao. 2003. Effects of methane partial pressure on synthesis of single walled carbon nanotubes by chemical vapor deposition. Journal of Materials Science 38: 3051- 3054.

Ward, D.A., E. I. Ko. Preparing Catalytic Materials by the Sol-Gel Method. 1995. Ind. Eng. Chem. Res. 34:421–433.

Wen, Q., W. Qian, F. Wei, Y. Liu, G. Ning, Q. Zhang. 2007. CO_2 assisted SWNT growth on porous catalysts. Chem. Mater. 19:1226-1230.

Wissler, M. 2006. Graphite and carbon powders for electrochemical applications. Journal of Power Sources 156: 142–150.

Xuan-ke, L., A. Westwood, A. Brown, R. Brydson, B. Rand. 2008. Wate assisted synthesis of clean single walled carbon nanotubes over a Fe_2O_3/Al_2O_3 binary aerogel catalyst. New Carbon Mater. 23(4):351-355.

Yacaman, M.J., M.M. Yoshida, L. Rendon, and J.G. Santiesteban. 1993. Catalytic growth of carbon microtubules with fullerene structure. Applied Physics Letters 62:202-207.

Yoshihara, N., H. Ago, M. Tsuji. 2007. Chemistry of Water-Assisted Carbon Nanotube Growth over Fe-Mo/MgO Catalyst. J. Phys. Chem. 111:11577-11582.

Yu, H., Q. Zhang, Q. Zhang, Q. Wang, G. Ning, G. Luo, F. Wei. 2006. Effect of the reaction atmosphere on the diameter of single-walled carbon nanotubes produced by chemical vapor deposition. Carbon 44: 1706-1712.

Yudasaka, M., R. Kikuchi, T. Matsui, O. Yoshimasa, and S. Yoshimura. 1995. Specific conditions for Ni catalyzed carbon nanotube growth by chemical vapor deposition. Applied Physics Letters 67:2477-2482.

Yudasaka, M., R. Kikuchi, Y. Ohki, E. Ota, and S. Yoshimura. 1997. Behavior of Ni in carbon nanotube nucleation. Applied Physics Letters 70:1817-1821.